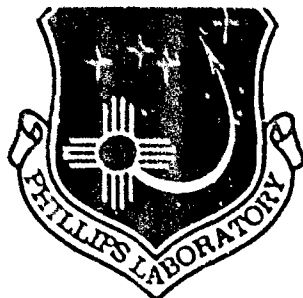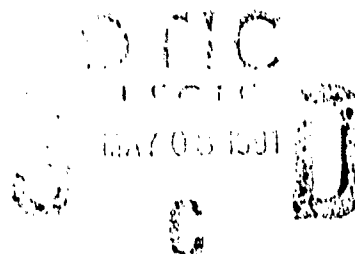# AD-A235 258

PL-TR-91-3002

AD:

Final Report
for the period
May 90 to
July 90

Engine Cycle Analysis for a

Particle Bed Reactor Nuclear

Rocket

March 1991

Author:
D. E. Suzuki

Approved for Public Release

Phillips Laboratory
Air Force Systems Command
Edwards AFB CA 93523-5000

91 5 07 125

REPORT DOCUMENTATION PAGE

Form Approved
OMB No. 0704-0188

1a. REPORT SECURITY CLASSIFICATION UNCLASSIFIED	1b. RESTRICTIVE MARKINGS
2a. SECURITY CLASSIFICATION AUTHORITY	3. DISTRIBUTION/AVAILABILITY OF REPORT Approved for Public Release; Distribution is Unlimited
2b. DECLASSIFICATION/DOWNGRADING SCHEDULE	

4. PERFORMING ORGANIZATION REPORT NUMBER(S) PL-TR-91-3002	5. MONITORING ORGANIZATION REPORT NUMBER(S)

6a. NAME OF PERFORMING ORGANIZATION Phillip's Laboratory	6b. OFFICE SYMBOL (If applicable) LSVF	7a. NAME OF MONITORING ORGANIZATION

6c. ADDRESS (City, State, and ZIP Code) OLAC PL/LSVF Edwards AFB, CA 93523-5000	7b. ADDRESS (City, State, and ZIP Code)

8a. NAME OF FUNDING/SPONSORING ORGANIZATION	8b. OFFICE SYMBOL (If applicable)	9. PROCUREMENT INSTRUMENT IDENTIFICATION NUMBER

| 8c. ADDRESS (City, State, and ZIP Code) | 10. SOURCE OF FUNDING NUMBERS |

PROGRAM ELEMENT NO.	PROJECT NO.	TASK NO.	WORK UNIT ACCESSION NO.
62302F	3058	00	R7

11. TITLE (Include Security Classification)

Engine Cycle Analysis for a Particle Bed Reactor Nuclear Rocket (U)

12. PERSONAL AUTHOR(S)
David E. Suzuki

13a. TYPE OF REPORT Final	13b. TIME COVERED FROM 90/05 TO 90/07	14. DATE OF REPORT (Year, Month, Day) 91/03	15. PAGE COUNT 63

16. SUPPLEMENTARY NOTATION

OLAC PL was formerly the Astronautics Laboratory (AFSC)

17.	COSATI CODES		18. SUBJECT TERMS (Continue on reverse if necessary and identify by block number)
FIELD	GROUP	SUB-GROUP	Mission Analysis, Nuclear Propulsion, Thermal Hydrolics
21	06		
21	08		

19. ABSTRACT (Continue on reverse if necessary and identify by block number)

This report addresses three candidate engine cycles for a particle bed nuclear rocket; (1) bleed cycle with uncooled carbon - carbon composite nozzle; (2) bleed cycle with regeneratively cooled Aluminum nozzle; (3) expander cycle with regeneratively cooled Aluminum nozzle. The analysis was performed using the SALT System Analysis Language Translator code with the following amendments; particle bed reactor was modeled as a simple heater; a regeneratively cooled nozzle model was added which includes the heating of the coolant due to hot exhaust gases and nuclear heating of nozzle. (The conclusion of the analysis were the topping cycle should be pursued for Mars missions and the bleed cycle should be pursued for OTV (Orbital Transfer Vehicle) missions.

This study indicates that a regeneratively cooled aluminum nozzle can be sufficiently cooled to allow its use with a PBR rocket engine. This result is based on nozzle heating due to hot exhaust gases at a maximum chamber temperature and nuclear heating effects. The highest temperatures occur at the nozzle throat, where a composite or alloy coating could protect the aluminum. Further investigation of nozzle cooling should include modeling the nozzle with

20. DISTRIBUTION/AVAILABILITY OF ABSTRACT ☒ UNCLASSIFIED/UNLIMITED ☐ SAME AS RPT. ☐ DTIC USERS	21. ABSTRACT SECURITY CLASSIFICATION UNCLASSIFIED
22a. NAME OF RESPONSIBLE INDIVIDUAL Lt Timothy J. Lawrence	22b. TELEPHONE (Include Area Code) 805-275-5640	22c. OFFICE SYMBOL LSVF

DD Form 1473, JUN 86   Previous editions are obsolete.   SECURITY CLASSIFICATION OF THIS PAGE

Block 19 (concluded)

more nodes, and including more accurate dimensions for the nozzle wall thicknesses and coolant flow passages.

The study also indicates that an expander cycle with a cooled aluminum nozzle can operate with a high pressure PBR at realistic TPA efficiencies. Further investigation should include the improvements to the regeneratively cooled nozzle model and more accurate performance maps for the TPA components.

The system modeling conducted in this study at steady-state indicates that for a possible manned mission to Mars an expander cycle with a cooled aluminum nozzle would minimize the initial mass in earth orbit required for the mission, and that for a LEO to GEO orbital transfer vehicle a hot gas bleed cycle with an uncooled carbon-carbon nozzle would maximize the useful payload delivered to geosynchronous equatorial orbit. Further analyses of engine cycles should include transient modeling of the cycles and a better model for the Particle Bed Reactor. Transient analyses may indicate other considerations, such as start-up time or failure modes, which may affect the engine cycle choice.

TABLE OF CONTENTS

DTIC
COPY
INSPECTED
6

Accession For
NTIS GRA&I   ☑
DTIC TAB   ☐
Unannounced   ☐
Justification

By
Distribution/

Availability Codes
Dist | Avail and/or
     | Special

A-1

iii

LIST OF FIGURES

LIST OF TABLES

APPENDICES

INTRODUCTION

This report analyzes possible engine cycles to be used with a Particle Bed Reactor (PBR) direct nuclear propulsion rocket system. Direct nuclear propulsion enables the achievement of very high specific impulses by heating a working fluid to high temperatures in a nuclear reactor and expanding the hot gas through an exhaust nozzle. The PBR has a much higher power density than current reactor designs, thus allowing the reactor to be smaller and lighter. This makes the PBR ideal for applications in space propulsion. The analyses are conducted for two possible missions: a low earth orbit (LEO) to geosynchronous equatorial orbit (GEO) orbital transfer vehicle (OTV) and a transfer vehicle for a manned mission to Mars.

This study indicates that a regeneratively cooled aluminum nozzle can be sufficiently cooled to allow its use with a PBR rocket engine. This result is based on nozzle heating due to hot exhaust gases at a maximum chamber temperature and nuclear heating effects. The highest temperatures occur at the nozzle throat, where a composite or alloy coating could protect the aluminum. Further investigation of nozzle cooling should include modeling the nozzle with more nodes, and including more accurate dimensions for the nozzle wall thicknesses and coolant flow passages.

The study also indicates that an expander cycle with a cooled aluminum nozzle can operate with a high pressure PBR at realistic TPA efficiencies. Further investigation should include the improvements to the regeneratively cooled nozzle model and more accurate performance maps for the TPA components.

The system modeling conducted in this study at steady-state indicates that for a possible manned mission to Mars an expander cycle with a cooled aluminum nozzle would minimize the initial mass in earth orbit required for the mission, and that for a LEO to GEO orbital transfer vehicle a hot gas bleed cycle with an uncooled carbon-carbon nozzle would maximize the useful payload delivered to geosynchronous equatorial orbit. Further analyses of engine cycles should include transient modeling of the cycles and a better model for the Particle Bed Reactor. Transient analysis may indicate other considerations, such as start-up time or failure modes, which may affect the engine cycle choice.

Why Use Nuclear Propulsion?

Direct nuclear propulsion is not a new idea, but was studied from 1955 to 1972 in the Nuclear Engine for Rocket Vehicle Applications (NERVA) test program. This program demonstrated the feasibility of direct nuclear propulsion and proved the capability of achieving very high specific impulses. The specific impulse (I_{sp}) of a rocket is defined as the thrust developed by the rocket divided by the weight flow rate of propellant. Therefore, a rocket with a high I_{sp} will need less fuel weight than a rocket with a lower I_{sp} to perform the same mission. This allows a greater percent of the initial mass of the rocket to be useful payload. The specific impulse of a rocket is directly proportional to the square root of the nozzle inlet temperature and inversely proportional to the square root of the propellant molecular mass (Ref. 1, 40). The I_{sp} of chemical rocket engines is limited by the relatively high molecular masses of the combustion products. Advanced liquid propellants and solid propellants have a maximum I_{sp} of about 475 seconds and 325 sec, respectively (Ref. 2, 1). However, since direct nuclear propulsion works by simply heating a working fluid in a suitable reactor, any gas can be used as a propellant. Hydrogen is an ideal candidate since it has the lowest molecular mass of any gas. Hydrogen engines can achieve an I_{sp} of 1000 sec or more at a temperature of 3000 Kelvin. Propulsion systems which do not use thermal expansion of a gas in a nozzle, such as electric propulsion, can achieve even higher specific impulses (4000–25000 sec) (Ref. 1, 31). However, the thrust level achievable by such systems is typically less than 1 Newton (Ref 1, 9) due to power supply limitations, resulting in extremely long trip times. Direct nuclear propulsion, though, is not limited in thrust. The increased performance of direct nuclear propulsion can be seen in Fig. 1. For a typical LEO to GEO transfer requiring approximately 14,000 ft/sec velocity change (Ref. 3) direct nuclear propulsion can place nearly twice as much payload as a liquid propellant rocket and three times the payload of a solid propellant rocket in GEO for the

same initial mass and assuming a single stage system. For a possible manned mission to Mars, which would require about 60,000 ft/sec Delta V (Ref. 3) the increased performance of direct nuclear propulsion could return well over ten times the payload to earth orbit than the most advanced chemical rockets for the same initial weight. Or, for the same payload weight, the chemical rocket would have to be more than ten times as massive at the beginning of the mission.
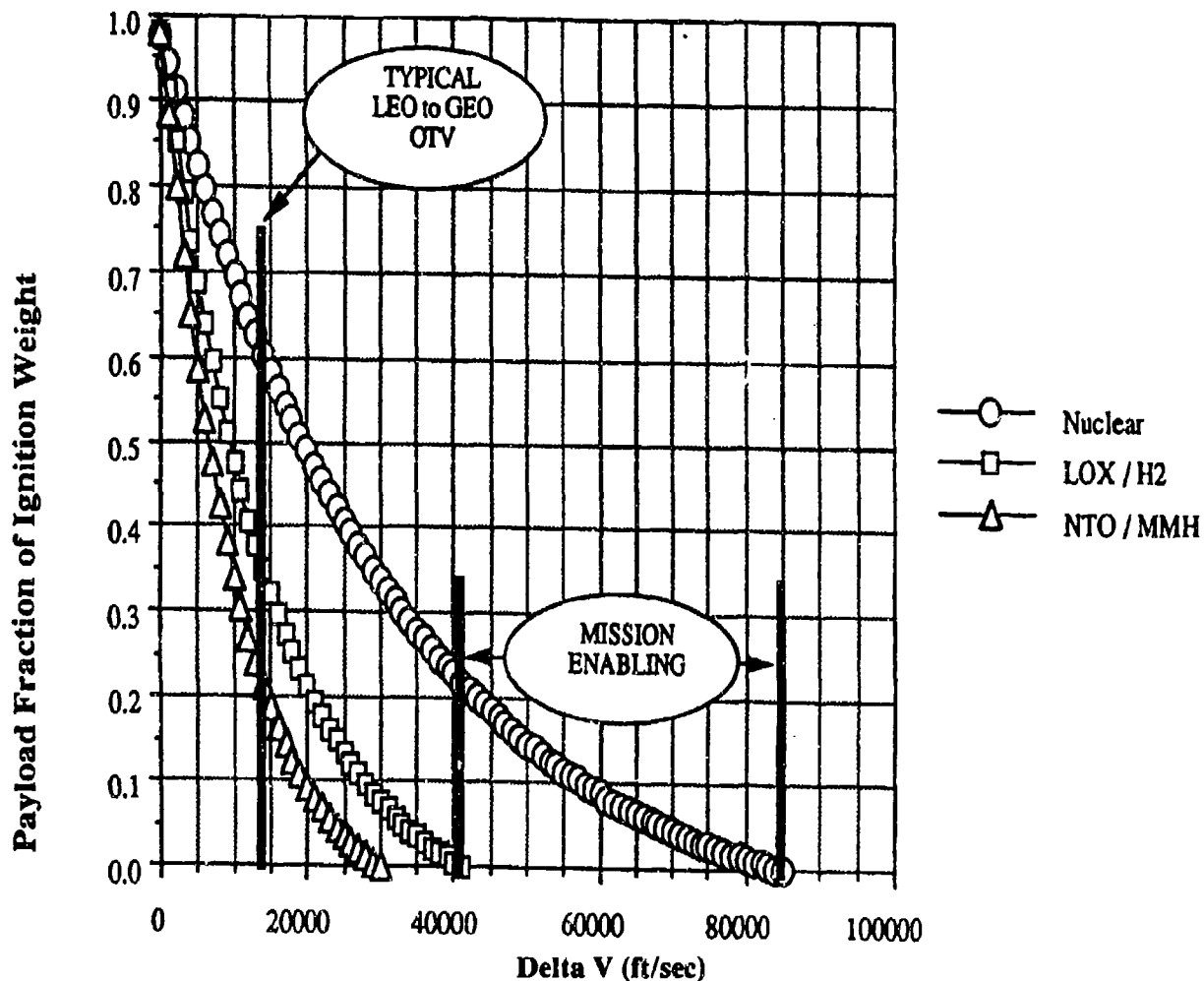
Fig. 1 Performance of Nuclear Propulsion

PROPULSION SYSTEM DESCRIPTION

Particle Bed Reactor Concept

The particle bed reactor is a nuclear reactor concept being designed by Brookhaven National Laboratory (BNL) (Ref. 4). Unlike the NERVA reactors in which the propellant flowed axially through long fuel elements consisting of uranium carbide kernels embedded in graphite, the propellant in a PBR flows radially through a porous bed of small fuel particles. This design has much more surface area per volume of fuel than the NERVA designs, which allows the heat from the fission process to be transferred more efficiently to the propellant, resulting in a higher power density. The PBR has an achievable power density of about 40 MegaWatts/liter compared to only 4 MW/l for the most advanced NERVA reactors. The high power density in turn greatly reduces the size of the PBR engine compared to the relatively large and heavy NERVA engines. This is the primary motivation for developing the PBR.

The PBR core consists of fuel elements (the number is dependent on the desired power level) arranged in a hexagonal pattern. The fuel elements are embedded in a moderator and contained within a pressure vessel. Each fuel element (Figs. 2 [Ref 10] & 3 [Ref 4]) is annular in shape with a 6.5 cm outside diameter. The bed of fuel particles is contained between two coaxial porous frits. The propellant flows into the inlet plenum from the surrounding channels and passes radially through the inlet or cold frit. The propellant is heated by the fuel particles and passes through the outlet or hot frit, which also forms the outlet plenum for the hot gas. The gas flows axially down the plenums and enters the exhaust nozzle.

Fig. 2 Fuel Element Design

Fig. 3 Baseline Fuel Element for Particle Bed OTV

There are several materials issues which must be addressed before the PBR can be built. The gas temperature needed to achieve 1000 sec I_{sp} is on the order of 3000 K, which is several hundred Kelvin above the temperatures in the NERVA reactors. The PBR, as well as other reactor designs, will need to incorporate materials which can withstand these high temperatures. In the PBR, the critical structure is the hot frits. A design requirement unique to the PBR is that the cold and hot frits will need to be both porous to allow the flow of the propellant and sufficiently strong to maintain the integrity of the fuel elements. The current design calls for the cold frit to be made of porous aluminum and the hot frit to be made of a carbon composite.

Exhaust Nozzle

Another area where material selection is a concern is the exhaust nozzle. The nozzle will not only be subjected to the hot gas exiting the PBR at approximately 3000 K, but will also be subjected to significant radiation heating due to its close proximity to the high power density reactor. BNL is currently considering using an uncooled carbon-carbon composite nozzle rather than a regeneratively cooled aluminum or aluminum alloy nozzle. This choice is based on the lighter weight and reduced complexity of an uncooled composite nozzle. In addition, analyses at BNL indicate that regenerative cooling may not be sufficient to keep the aluminum at an acceptable temperature due to higher nuclear heating of aluminum and its relatively low melting point (934 K). However, it has not yet been demonstrated that a carbon-carbon nozzle can withstand the high temperature exhaust gases without significant regression of the nozzle material. This report analyzes engine cycles using both aluminum and carbon-carbon nozzles.
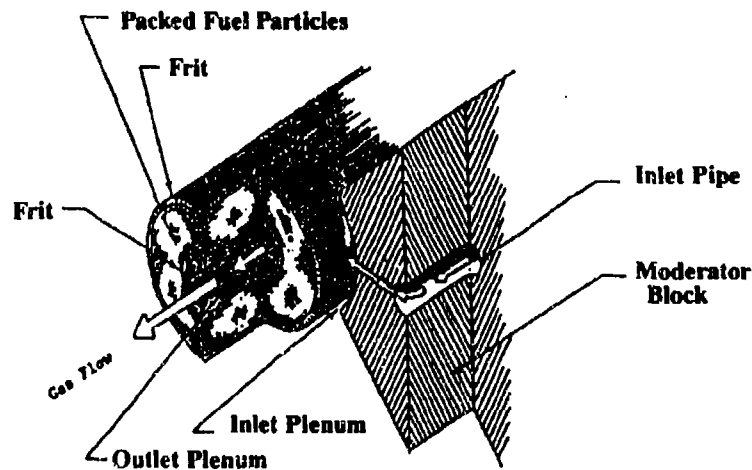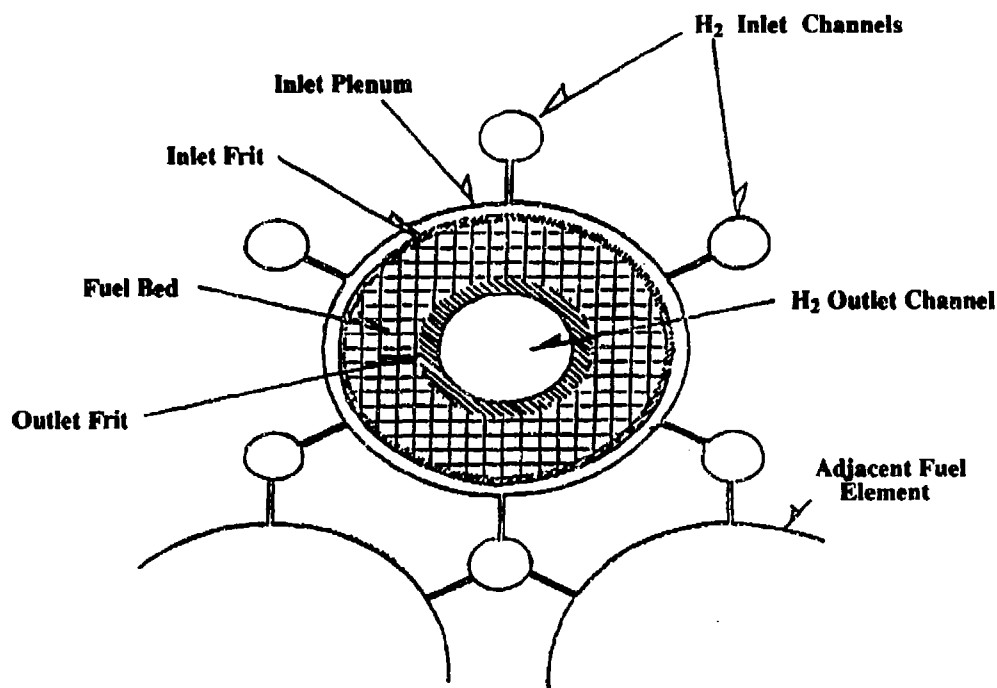
- 4 -

Fig. 3 Baseline Fuel Element for Particle Bed OTV

There are several materials issues which must be addressed before the PBR can be built. The gas temperature needed to achieve 1000 sec I_{sp} is on the order of 3000 K, which is several hundred Kelvin above the temperatures in the NERVA reactors. The PBR, as well as other reactor designs, will need to incoiporate materials which can withstand these high temperatures. In the PBR, the critical structure is the hot frits. A design requirement unique to the PBR is that the cold and hot frits will need to be both porous to allow the flow of the propellant and sufficiently strong to maintain the integrity of the fuel elements. The current design calls for the cold frit to be made of porous aluminum and the hot frit to be made of a carbon composite.

Exhaust Nozzle

Another area where material selection is a concern is the exhaust nozzle. The nozzle will not only be subjected to the hot gas exiting the PBR at approximately 3000 K, but will also be subjected to significant radiation heating due to its close proximity to the high power density reactor. BNL is currently considering using an uncooled carbon-carbon composite nozzle rather than a regeneratively cooled aluminum or aluminum alloy nozzle. This choice is based on the lighter weight and reduced complexity of an uncooled composite nozzle. In addition, analyses at BNL indicate that regenerative cooling may not be sufficient to keep the aluminum at an acceptable temperature due to higher nuclear heating of aluminum and its relatively low melting point (934 K). However, it has not yet been demonstrated that a carbon-carbon nozzle can withstand the high temperature exhaust gases without significant regression of the nozzle material. This report analyzes engine cycles using both aluminum and carbon-carbon nozzles.
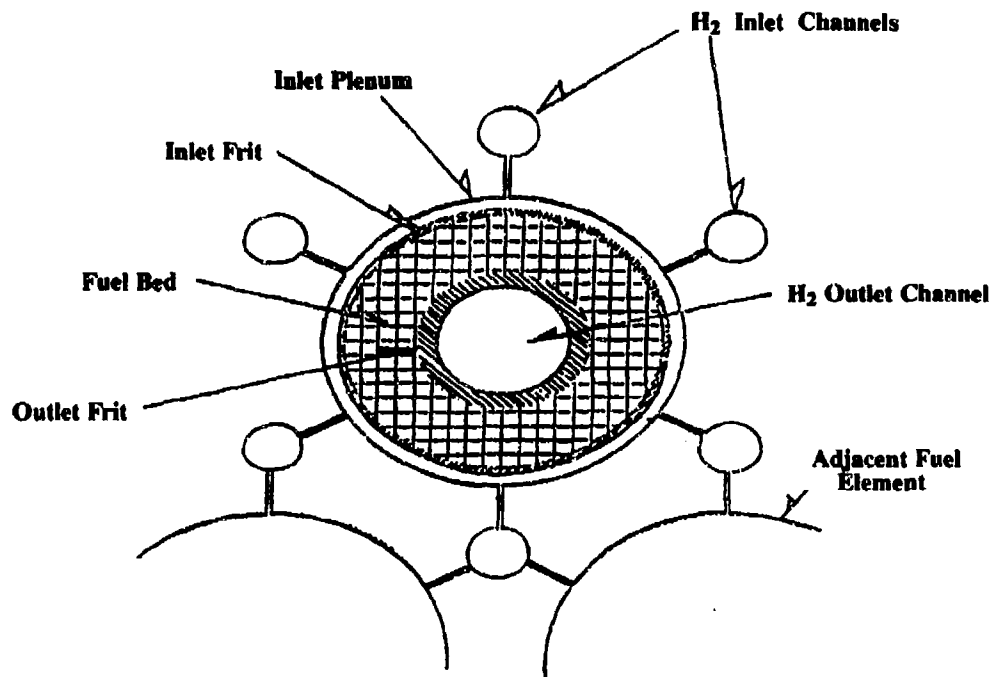
Propellant

As previously discussed, hydrogen provides the highest possible specific impulse of any gaseous propellant. Therefore, hydrogen is the current propellant of choice for the PBR rocket, and will be used in the analyses in this report. The hydrogen will need to be stored as a liquid at cryogenic temperatures, and due to its low density, the necessary propellant tanks will need to be quite large, especially for a Mars mission. Other propellants which are easier to store such as carbon dioxide, methane, ammonia, or even water could also be used. In order to reduce the amount of propellant needed for the Mars mission, it is theoretically possible to take advantage of the flexibility of direct nuclear propulsion by refueling at Mars with carbon dioxide, the primary component of the Martian atmosphere. Carbon dioxide would deliver a smaller I_{sp}, but its use would eliminate the need to take enough fuel for a round trip. Other issues exist in using CO_2 (and other propellants), though, such as coking of any carbon components and oxidation of components due to the dissociation of the carbon and oxygen at the high temperatures in the PBR. Therefore, in order to use CO_2 or other gases as a propellant, the reactor components would have to be redesigned.

Power Level

One of the initial BNL PBR designs for a hydrogen rocket OTV was a 19 element 150 $MW_{thermal}$ reactor with a propellant mass flow rate of 3.8 kg/sec and a reactor inlet pressure of 61 atmospheres (Ref. 4, 131). These are the baseline parameters to be used for the analysis of the LEO to GEO OTV mission. Scale-up of the OTV design parameters for a possible Mars mission would require 37 fuel elements producing a 2000 MW_t reactor with a propellant flow rate of about 40 kg/sec. The final propellant temperature for both power levels is designed to be 3000 K (Ref. 5).

ENGINE CYCLES

The overall goal of an engine cycle is to insure the proper flow of propellant through the heating device. For engines operating at high mass flow rates or high pressures, a turbopump is almost always used to increase the propellant pressure from its storage value to the necessary chamber pressure. Power to run the turbopump is most often provided by a gas turbine operating on part of the propellant flow. The engine cycles which can be used with a PBR are limited because of the absence of combustible propellants; gas generators or pre-combustors cannot be used to provide the high energy gas needed to run the turbine. There are two basic engine cycles which can be used with a PBR: the hot gas bleed cycle and the topping or expander cycle.

Hot Gas Bleed Cycle

The hot gas bleed cycle operates the turbopump assembly (TPA) by bleeding off a small amount of hot gas from the chamber (reactor) outlet and expanding it through a high pressure ratio gas turbine. Since the gas at the turbine outlet will necessarily be lower in pressure than the reactor inlet pressure, the hot gas exiting the turbine cannot be fed back into the reactor, and must be exhausted into space. This is the primary drawback of the bleed cycle since a small percentage of the propellant is not expanded through the main nozzle, thus reducing the overall specific impulse and thrust of the rocket engine. This engine cycle can be operated with either an uncooled or a cooled nozzle, so it is compatible with both the carbon-carbon and aluminum nozzle designs.

Uncooled Nozzle

Fig. 4 shows a schematic diagram of a bleed cycle with an uncooled nozzle. The liquid hydrogen propellant is pumped to the reactor inlet pressure. The flow is split with the majority of the flow entering the PBR. A majority of that flow is then expanded through the nozzle. A small amount of flow is bled from the reactor outlet and mixed with a small amount of cold flow. This is to keep the temperature at the gas turbine inlet below the failure point for the blade material. This gas is then expanded through the turbine and exhausted to space.
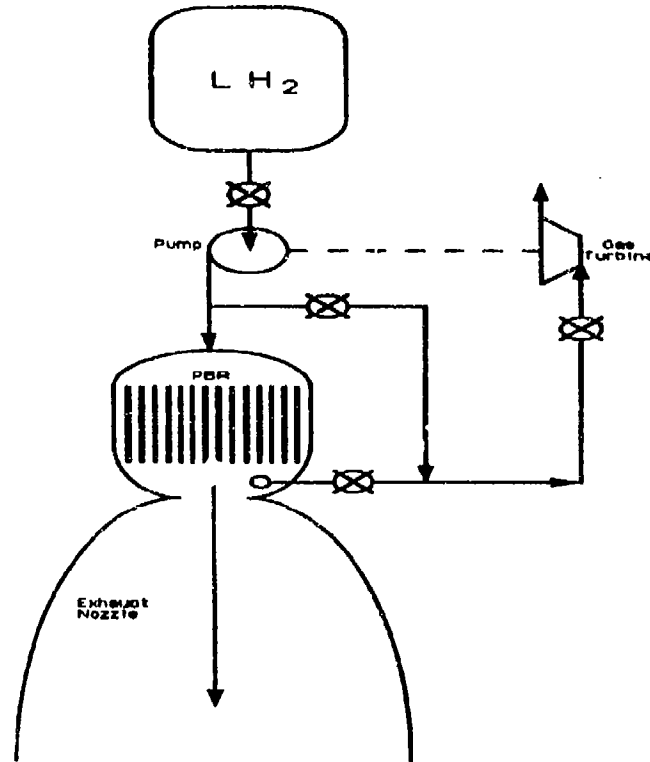
Fig. 4 Hot Gas Bleed Cycle (Uncooled Nozzle)

Cooled Nozzle

Fig. 5 shows a schematic for a bleed cycle with a regeneratively cooled nozzle. The propellant is first pumped to the reactor inlet pressure. The flow is split and part enters the PBR. The remaining flow is pumped to a higher pressure and fed through the cooling jacket of the nozzle. The pressure loss of the fluid through the cooling jacket should equal the pressure rise of the second pump. This flow is split and most is mixed with the cold flow and fed into the reactor. The remaining flow is mixed with hot gas bled from the reactor outlet to reduce its temperature and expanded through the gas turbine. The main flow through the reactor is expanded through the main exhaust nozzle.

Expander Cycle

The expander cycle operates by heating part or all of the cold propellant in a regeneratively cooled nozzle. This hot gas is then used to run the gas turbine. If a low pressure ratio turbine is used and the propellant passing
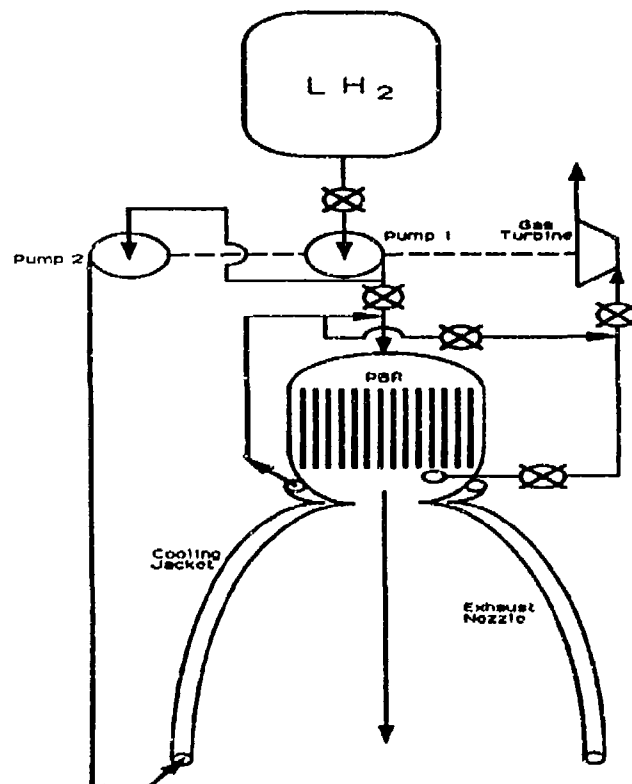
Fig. 5 Hot Gas Bleed Cycle (Cooled Nozzle)

through the cooling jacket is first pumped to a pressure sufficiently above the chamber pressure, the gas exiting the turbine can be fed into the reactor with the rest of the propellant. This means that the entire propellant flow will be fully expanded through the nozzle, maximizing the thrust and specific impulse. Since this cycle uses the energy gained in the cooling jacket to operate the TPA, it cannot be used with an uncooled carbon-carbon nozzle, but only with the cooled aluminum nozzle. There are two key issues concerning an expander cycle which need to be addressed in this study. First, can enough enthalpy be gained in the cooling jacket to power the TPA, and second, can the nozzle be sufficiently cooled by the propellant to prevent failure. Fig. 6 shows a schematic of the expander cycle. The propellant is first pumped to the reactor inlet pressure. The flow is split and the main flow enters the reactor. The remainder of the flow passes through a second pump and enters the nozzle cooling jacket. The hot gas is then expanded through the gas turbine. The pressure losses in the cooling jacket and turbine should equal the pressure rise in the second pump. The gas exiting the turbine is then fed into the PBR with the cold gas. The entire flow through the reactor is then expanded through the exhaust nozzle.
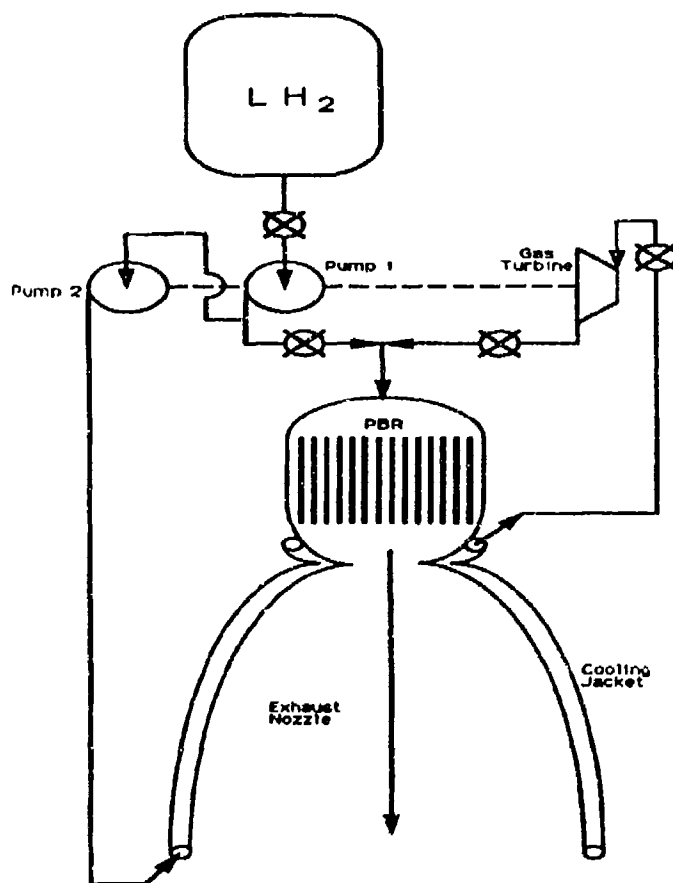
Fig. 6 Expander Cycle

ANALYSIS APPROACH

In order to analyze the performance of the different engine cycles it was necessary to find a way to accurately model the thermodynamics of the systems. The System Analysis Language Translator Code (SALT) (Ref 6) developed by Argonne National Laboratory (ANL) for use in analyzing fossil fuels and adapted by the Phillips Laboratory (PL) for rocket engine systems was chosen. The SALT code uses a modular approach which allows the flexibility of modeling different systems by simply rearranging the order of the modules and also allows the user to add new modules. There are two versions of the SALT code. The first is designed for steady-state analyses and the other is designed for dynamic analyses. While the analyses in this report are conducted at steady-state, the dynamic version of SALT was chosen. This version has more complex and accurate models than the steady-state code, and has the ability to operate in a steady-state mode.

The SALT Code

The SALT code is written in C+ + and makes extensive use of the C+ + concept of classes. A class is simply a data structure containing data and functions to manipulate the data (Ref. 6, 2). There are four types of classes used in the dynamic version of SALT. The class types are mathematical utility classes, flow type classes, shaft type classes and model classes. The mathematical utility classes are used to set up system constraints, optimizations, and ordinary differential equations. The flow type classes are used to save and transfer the gas flow properties between the model classes. The shaft type classes do the same for models which have a shaft input or output such as a pump or gas turbine. The model classes are used to simulate the individual components of the rocket system. The dynamic model classes which were available at the start of this study are very briefly discussed below (the C+ + class name is in capital letters). The GAS model is used to initiate a gas flow at specified conditions. The type of gas must also be specified so that its thermodynamic properties can be retrieved. The properties used for this study were from the Joint Army, Navy, NASA, Air Force (JANNAF) database which uses equations of state. The SHaFT model initiates a shaft flow for use with work producing or consuming models. The SPlitter model splits a flow into two separate flows. The split ratio can be fixed or allowed to vary to meet some system constraint. The MiXer model combines two flows. The flows are constrained to be the same pressure in the steady-state mode since a low pressure flow could not flow into a higher pressure region. The Heater model transfers heat into or out of a gas flow. The REACtor model simulates a very general pin-type reactor and is primarily just a heat exchanger. The Gas Turbine model works as a simple expansion device for the flow and produces work to drive the shaft. The expansion is at a given pressure ratio and efficiency. The ComPressor models a gas compression process at a given pressure ratio and efficiency and consumes work. The PUMP model consumes work to increase the pressure of a liquid flow by a given pressure rise. The gas turbine, compressor, and pump require performance maps to operate. Generic data maps provided by ANL were used in this study. The PIpe model simulates flow through a pipe. The VALVe models a simple valve with a given pressure drop. The MOTor and GENerator models represent a motor and generator. The CoNTroLler model simulates a proportional-integral-derivative controller which can be used to control a variable of some other model. The EXhaust NoZzle models the expansion of flow through a nozzle with a given efficiency. The model also calculates the thrust and specific impulse developed by the nozzle.

SALT Code Amendments

As previously discussed, one of the advantages of using the SALT code is the ability to easily add or change model classes to suit the particular needs of the user. This was accomplished in order to better model the engine cycles to be used with the PBR.

Exhaust Nozzle

The exhaust nozzle model originally calculated the exit area based on a desired exit pressure. It was decided that the expansion ratio of the nozzle would be a better input parameter. This allows the user to model the nozzle based on its size and not a performance characteristic. In the steady-state mode, the throat area is still calculated to produce sonic (choked) flow at the throat. The exit area is then found by simply multiplying the expansion ratio by the throat area.

PBR

The SALT code does not have an accurate representation of the PBR. Developing a model of the thermohydraulics of the PBR was beyond the scope of this study. In fact, the complete thermohydraulics modeling is still under development by BNL. The major issue in the model development is the large degree of coupling among the system components, so that a large number of iterations are necessary. In test runs using the available reactor

model, the fuel temperature rose to unreasonable levels (ten times the coolant temperature), so the reactor model was eliminated as even a rough model. Since temperature is the overriding determinant of the specific impulse for a given propellant and exhaust nozzle, it was decided that as long as the PBR outlet temperature could be specified, the model would be sufficient for the purposes of this study. The propellant exit temperature from the PBR is essentially independent of the reactor inlet conditions, (Ref . 5) so a simple heater model was used. The heater model from the steady–state version of SALT was chosen over the dynamic model due to the ability to simply input the final propellant temperature.

Regeneratively Cooled Nozzle

The SALT code did not have the ability to simulate the flow of propellant through a regeneratively cooled nozzle beyond a simple heater or heat exchanger. As previously mentioned, the engine cycle analysis is heavily dependent on the performance of the cooled nozzle, so it was decided to create a new model class for the simulation. The new class name is RGEN and its computer code is listed in Appendix A.

The model is designed to simulate the heating of coolant in a counter flow cooling jacket due to the hot exhaust gas flow and also nuclear heating of the nozzle. The methodology of this model was adapted from a regeneratively cooled nozzle model in the Expanded Liquid Engine Simulation (ELES) Computer Program (Ref. 7). The model divides the nozzle into twelve nodes – two above the throat and ten below the throat – to simplify the analysis. The model requires that some information be known about the nozzle at each node before it can be implemented. This information includes the nozzle shape (expansion ratios and surface areas) and heat transfer coefficients on the hot gas side. Other nozzle information needed is the wall thickness between the hot gas and the coolant, the thermal conductivity of the nozzle material, the nuclear heating rate in the nozzle, the maximum possible coolant side heat transfer coefficient, the maximum allowable nozzle temperature, and the pressure drop through the cooling jacket.

The model first calculates the needed coolant side heat transfer coefficients to maintain the nozzle at its maximum allowable temperature for a specified maximum chamber temperature. This temperature should be well above the full power design temperature to establish a factor of safety in the nozzle design. The necessary heat transfer at each node is calculated by setting the gas wall temperature to the maximum allowable value. The gas temperature at the node is determined from isentropic flow relations. These temperatures along with the gas side heat transfer coefficient (h_g) specify the convective heat transfer across the gas side boundary layer according to the equation:

$$q = h_g \left(T_{gas} - T_{wall-gas} \right) \qquad\qquad 1.$$

Radiative heat transfer from the exhaust gases to the nozzle are assumed to be insignificant. This same heat must then be conducted across the nozzle wall. Since the thermal conductivity (k), wall thickness (l), and gas side wall temperature are known, the coolant side wall temperature is specified for the given heat transfer rate from:

$$q = k/l \left(T_{wall-gas} - T_{wall-coolant} \right) \qquad\qquad 2.$$

The coolant temperature at the node is assumed to be uniform and equal to the cooling jacket inlet temperature for the first node, and the exit temperature from the previous node thereafter. The coolant side wall temper-

ature, coolant temperature, and heat transfer rate specify the necessary coolant side heat transfer coefficient (h_l) from:

$$q = h_1 (T_{wall-coolant} - T_{coolant}) \qquad\qquad 3.$$

A similar process is conducted for the necessary cooling of the nuclear heating inputs to the nozzle. It is assumed that nuclear heating will be uniform throughout the nozzle and that the effects can be calculated independently from the exhaust gas heating. The magnitude of the nuclear heating can be found from computer models such as the FEMP2D (Finite Element, Multigroup, P_n, 2-Dimensional) code developed by Sandia National Laboratory. The coolant side wall temperature is set to the maximum allowable wall temperature, and the heat transfer rate can be calculated from the nuclear heating rate per volume and the surface area to volume ratio for the nozzle material. The necessary coolant side heat transfer coefficient is then specified. The larger of the two heat transfer coefficients is taken to be the design value. These values are actually determined by the coolant channel geometry, so the values specify the design requirements. If the needed heat transfer coefficients exceed the maximum value which can be designed, the maximum value must be used, and the nozzle will not be sufficiently cooled. If this is the case, the model will calculate the maximum temperature the nozzle will reach and print an appropriate warning message. Finally, the heat transfer rate into the coolant, the surface area (A_{surf}) available for heat transfer, the coolant specific heat (C_p), and the coolant mass flow rate (m) is used to calculate the temperature rise for that node by:

$$\delta T = \frac{(q_{gas} + q_{nuc}) (A_{surf})}{(C_p)(m)} \qquad\qquad 4.$$

The model next calculates the exit conditions of the coolant for the actual operating conditions. An initial guess of the chamber temperature must be input, but the value used can be forced to match the chamber temperature by using the mathematical utility classes available. This can be accomplished by allowing the assumed chamber temperature to vary and constraining it to equal the actual chamber temperature. The design values of the coolant side heat transfer coefficients are then used to determine the heat transfer rate from the hot gas at each node by the equation:

$$q = \frac{(T_{gas} - T_{coolant})}{(1/h_g) + (1/k) + (1/h_1)} \qquad\qquad 5.$$

The heat transfer rate due to nuclear heating is the same as in the first part of the model. These values are then used to determine the temperature rise at each node. The gas temperature at the cooling jacket exit is therefore specified. The pressure drop of the propellant through the cooling jacket is determined by simply specifying the drop as a fraction of the inlet pressure. This is due to the complexity of trying to calculate an actual pressure loss at each node. Values based on previous experience or probable worst case approximations should suffice for most applications. The exit temperature and pressure completely specify the thermodynamic state, and the other properties are determined by referencing the thermodynamic database for the particular propellant.

ENGINE CYCLE MODELING

This section describes specifically the modeling process for the individual engine cycles. The creation of the necessary computer coding and an explanation of the input parameters are discussed for each cycle.

Bleed Cycle (Uncooled Nozzle)

The hot gas bleed cycle with an uncooled carbon–carbon nozzle was shown in Fig. 4. The equivalent schematic diagram using the model classes available with the SALT code is shown in Fig. 7. The boxes in Fig. 7 are the different model classes which simulate the physical components of Fig. 4. The solid lines show the transfer of gas type flows between the model classes, and the dashed lines show the transfer of shaft type flows. The only difference in the two diagrams is the inclusion of the shaft model class needed to initiate a shaft flow in the SALT coding. The computer code derived from the block diagram is shown in Appendix B for the 2000 MW PBR and Appendix C for the 150 MW PBR.
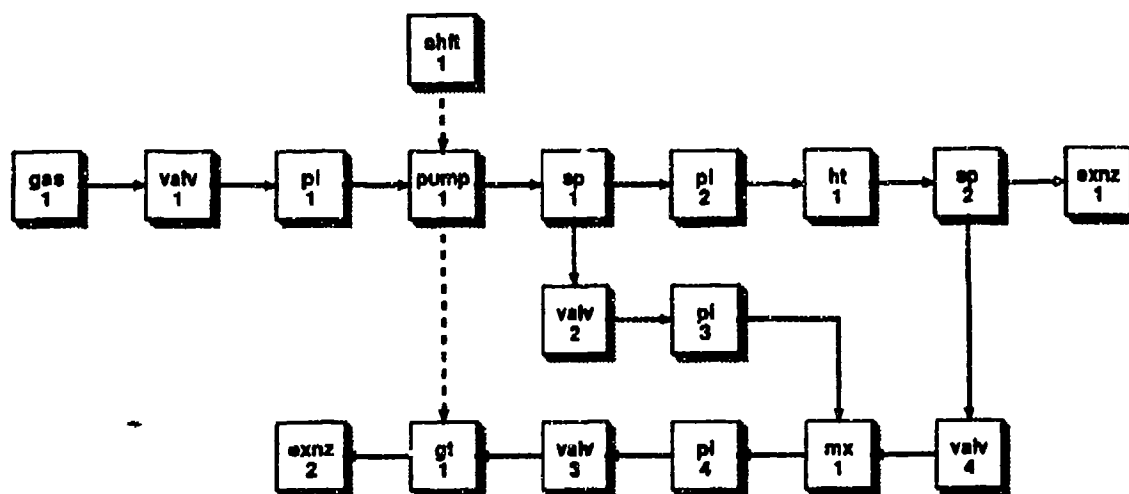
Fig. 7 Bleed Cycle (Uncooled Nozzle)

2000 MW PBR

The first four lines of code are common to all the simulations in this study. The first line indicates which file the model classes are defined in. The next line creates a conversion factor between Pascals and atmospheres. The third line defines two task loops for use with the mathematical utility classes, and the fourth line defines the flow type classes. The first part of the code under the main program defines the input parameters to the model classes. If values are not specified, default values specified in the individual model codes will be used.

The gas_1 model is used to initiate the gas flow. The parameters (named in parentheses) indicate that the fluid is hydrogen (id) at 20 K (t) and 0.1 MPa (p). The flow rate is 40 kg/sec (m). The quality (q) of the fluid is 0.0 which

indicates a saturated liquid. The tank exit is 0.1 m in diameter (diam). The flow velocity (v) is defined, but is actually calculated from the flow rate, density, and tank exit area. The stat equal to 1 indicates that the model class is operating in a steady state mode, so the mass flow rate is fixed at the given value.

The valv_1 model represents the tank shut-off valve. The pressure drop is set to 0.01 which means a pressure drop of 1% of the inlet pressure. The low pressure drop indicates that the valve is essentially fully open.

The pi_1 model is simply a pipe connecting the valve to the pump. The num parameter equal to zero indicates that thermal delays along the length of the pipe will be ignored. The model represents one parallel pipe (num_par). The pressure drop through the pipe at the rated mass flow rate (rat_m) of 40 kg/sec is 0.01% of the inlet pressure (rat_pf). The pipe length is 1.0 m, which is not used in calculations at steady-state. The pipe diameter (diam) of 0.1 m was set to keep the flow velocity at a reasonable value.

The pump_1 model represents a pump with a rated pressure rise (rat_dp) of 6.0 MPa at the design mass flow rate (rat_m) of 40 kg/sec. The pump operates at 60000 rpm (rat_rpm) at steady-state with an efficiency (rat_eff) of 70%. The pump polar moment of inertia (inertia) is 0.1 kg/m^2.

The pi_2 model, and subsequent pipe models are the same as the first one, with a rated mass appropriate for that branch of the fluid flow, and a diameter to maintain the flow at reasonable velocities.

The htss_1 model is the heater model taken from the steady-state version of SALT to simulate the temperature rise in the PBR. The flow exit temperature (temp) is 3000 K as previously discussed. The pressure drop through the PBR (pfrac) is expected to be about 5% (Ref 5).

The sp_2 model represents the bleeding of hot gas from the reactor outlet plenum. The split ratio (sr) is set to an initial guess of 0.01, meaning that the secondary output flow will have 1% of the inlet mass flow rate. The diameters are set as with the pipe diameters, with [0] being the primary flow and [1] the secondary flow. The stat option equal to zero indicates that the split ratio will be automatically varied to meet some system constraint.

The exnz_1 model simulates the main exhaust nozzle. The nozzle has an 85% efficient (eff) expansion process and an area ratio (ratio) of 125:1. The stat option equal to zero indicates that the model will vary the throat area to produce choked flow at the throat for the given mass flow rate.

The valv_2 and subsequent valve models are similar to the first. In the case of valv_2, the pressure drop is larger since it will later be varied to meet a system constraint.

The mx_1 model represents the mixing of the hot and cold gas flows before it enters the gas turbine. The stat option equal to 1 indicates that the model will impose a constraint on the system that the two inlet flows be of equal pressure.

The gt_1 model simulates a gas turbine with an expansion ratio (rat_pr) of 10 and an efficiency (eff) of 80%. The stat option equal to 1 indicates that the model is operating at steady-state.

The exnz_2 model differs from the first in that its area ratio is 1.0, indicating it does not have a divergent section. This is because this nozzle is simply to dump the low pressure turbine exhaust into space, and is not designed for thrust.

The sp_1 model represents the splitting of cold gas to be mixed with the hot bleed gas. The split ratio is varied to maintain the gas turbine inlet temperature at a reasonable level.

The shft_1 model initiates the shaft type flow at a speed of 60000 rpm.

The next line opens the performance map files for use with the pump and gas turbine models. The next line begins the sta task loop, which iterates over the system variables in order to meet any system constraints. The first line of the sta task loop sets the option for printing the loop variables and sets the accuracy for convergence. The loop will repeat until the variables converge, exceed specified bounds, or the number of iterations exceed 40. The first line within the loop creates the first system variable. The valv_2 pressure drop will be varied from 2% to 17% in order to meet the automatically imposed mixer constraint. The next two variables are the split ratios which are automatically varied. The corresponding constraints appear at the end of the loop. The first split ratio is constrained so that the gas turbine inlet pressure is 1300 K. This value was chosen as a conservative value to prevent material failure of the turbine blades. The second split ratio controls the mass flow through the turbine, and is constrained so that the power produced by the gas turbine equals the power consumed by the pump. The series of statements in the middle of the loop are the call statements for the model classes. It is the order of these statements which create the different engine cycles. The .s calls indicate the secondary output flow for a splitter or the secondary input flow for a mixer model. The final line is used to print the results of the simulation.

150 MW PBR

The modeling of the bleed cycle with a carbon-carbon nozzle for the small PBR to be used for an OTV is very similar to the larger PBR model. The differences are that the mass flow rates are scaled down to 3.8 kg/sec from 40 kg/sec, and the diameters of passages are scaled down appropriately for the smaller flow rates. In addition, the shaft speed was changed to 30000 rpm.

Bleed Cycle (Cooled Nozzle)

The schematic diagram of a bleed cycle with a regeneratively cooled aluminum nozzle was shown in Fig. 5. The corresponding block diagram is shown in Fig. 8. The computer codes appear in Appendices D and E for the 2000 MW and 150 MW reactors, respectively. The two power levels will be discussed together and only significant changes from the previous cycle will be discussed.
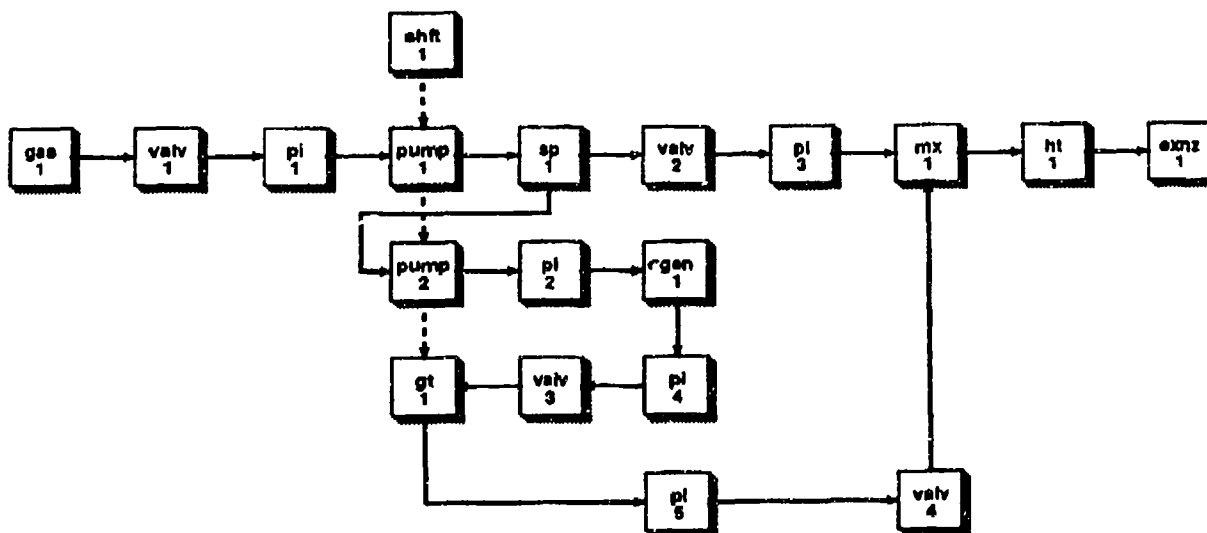
Fig. 8 Bleed Cycle (Cooled Nozzle)

This system includes a sp_3 model which splits a portion of the propellant flow to be passed through the cooling jacket (rgen_1). The split ratio allows 30% of the flow to pass through the cooling jacket and was not varied since there was not an additional system constraint. This flow pressure is then increased an additional 4.0 MPa in pump_2 to overcome pressure losses through the cooling jacket. The input to the rgen_1 model was quite complex. The maximum chamber temperature is taken as the default value of 3500 K. The initial guess for chamber temperature (tc) was 3000 K. The maximum allowable wall temperature (twmax) was set to 780 K, which BNL chose as the maximum safe operating temperature for aluminum. The wall thickness on the gas side of the coolant (lw) was chosen to be 0.25 cm. The rated pressure drop (rat_pf) through the jacket at the design mass flow was conservatively chosen to be 40% of the inlet pressure. This value is typical for very high pressure cooling jackets (Ref. 3). The stat option equal to 1 indicates that the design mass flow will be determined by the actual mass flow. The nuclear heating rate for an aluminum nozzle has been found by AL using the FEMP2D code to be approximately 20 W/cm3 for a 400 MW PBR. This value was scaled linearly to produce a heating rate of 100 W/cm^3 for the 2000 MW PBR and 7.5 W/cm3 for the 150 MW PBR. For both power levels it was assumed that the space side nozzle wall would be 1 cm thick, so that for each square cm of surface area there is 1.25 cm^3 of nozzle volume. Therefore the necessary heat transfer rate (q_nuc) is 1250 kW/m^2 for the 2000 MW PBR and 93 kW/m^2 for the 150 MW PBR. The nozzle size (area ratio [ar] and surface area [surf]) and gas side heat transfer coefficients (hg) at each node are determined from those calculated by BNL (Figs. 9 & 10 [Ref. 4]). For the 150 MW$_t$ OTV mission the data was taken directly from the graphs at 10 cm intervals. For the scaled-up 2000 MW$_t$ Mars mission, the nozzle shape was left unchanged, but the throat area was designed to be 11 times the throat area for the OTV nozzle since the mass flow rate is about 11 times as large. The surface areas at the nodes, therefore, were also increased by a factor of 11. The heat transfer coefficients at each node were assumed to be the same as for the smaller nozzle since the nozzle geometry was unchanged. While the actual values would probably decrease slightly due to the reduction in the surface area to volume ratio, it was felt that since the heat transfer coefficients can only be determined empirically, little accuracy would be gained by changing the values. The determination of the maximum possible coolant side heat transfer coefficient was based on limiting the flow velocity through the cooling jacket to 0.2 Mach. The appropriate calculations are shown in Appendix F. The value calculated for hlmax is 225 kW/m^2-K for the large nozzle, and the same value is assumed for the small nozzle.
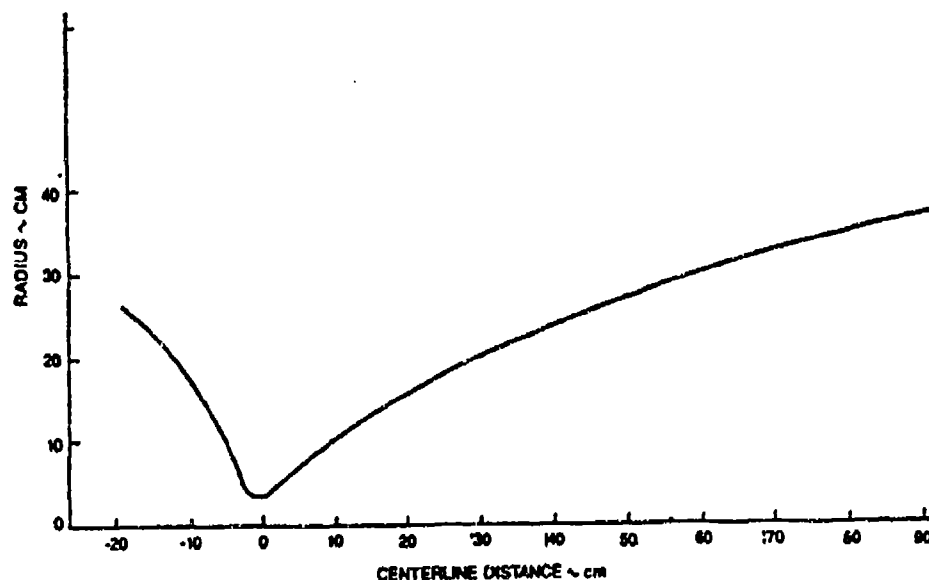
Fig. 9 Nozzle Contour

- 15 -
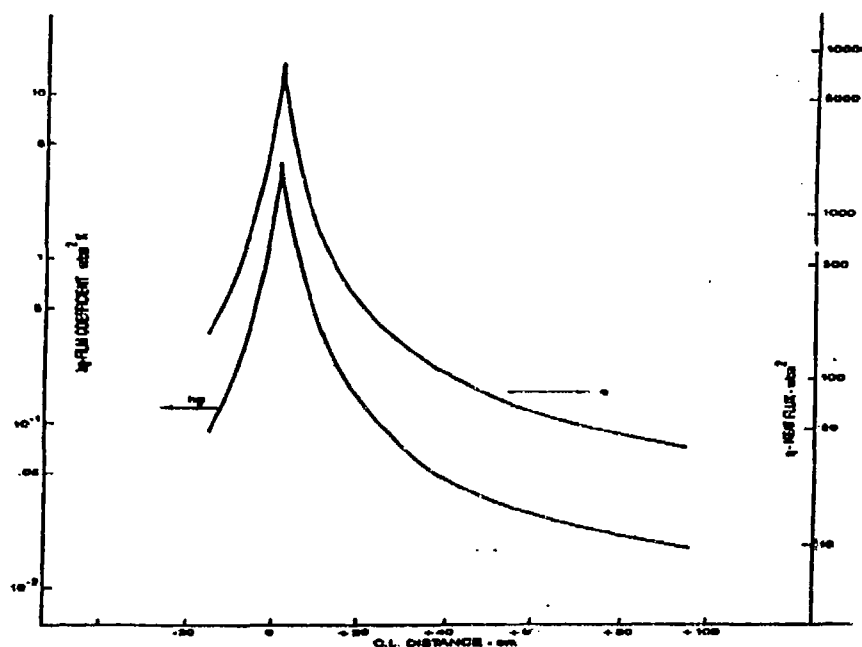
Fig. 10 Heat Transfer Coefficients

The variables for the sta task loop are the pressure drop for valv_2 and valv_5. These are both used to meet the two mixer model constraints. The other constraints were again the gas turbine inlet temperature and the power balance, this time for the gas turbine and both pumps.

Expander Cycle

The expander cycle was shown in Fig. 6, and the corresponding block diagram is shown in Fig. 11. The computer codes are listed in Appendices G & H for the 2000 MW and 150 MW PBR, respectively.

The key difference in the expander cycle is that the gas exiting the turbine is not exhausted to space but is mixed with cold gas and enters the PBR. In order to accomplish this, the gas turbines must have a low pressure ratio but high mass flow rate. For the 2000 MW PBR, the gt_1 model has a pressure ratio of 2.0 and a mass flow rate of 30% of the total flow. The split ratio for the cooling jacket was varied manually since the computer had difficulty constraining the power production to equal the power consumption. The necessary pressure ratio in the second pump was 14.0 MPa, bringing the total pressure at the cooling jacket inlet to about 200 atmospheres. While this seems high, it is not uncommon (Ref. 3). For the 150 MW reactor, the gas turbine pressure ratio is 1.5 with 50% of the total flow. The second pump has a pressure rise of 9.0 MPa. The cooling jacket parameters are the same as for the bleed cycle with a cooled nozzle.

The valv_2 pressure drop is varied to meet the mixer constraint. The one split ratio is not varied, as previously discussed, so there is no constraint on the power balance. A vary/constrain pair is added to force the assumed chamber temperature in the rgen_1 model to equal the actual flow temperature exiting the reactor. However, since the reactor outlet temperature is always 3000 K, the constraint is already met.
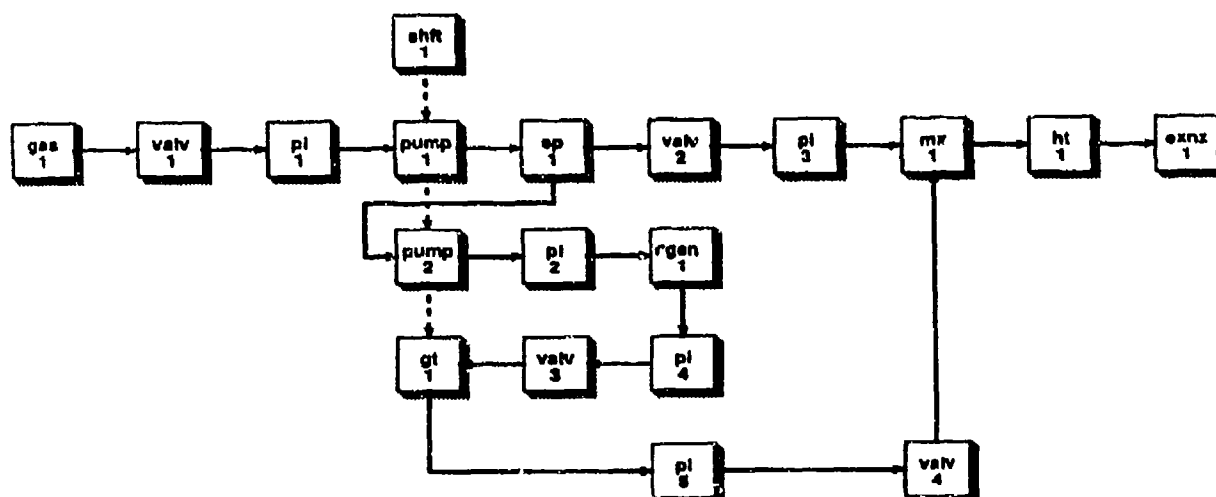
Fig. 11 Expander Cycle

SIMULATION RESULTS

The complete computer output for each of the six engine cycle cases is listed in Appendices I – N. The output has three sections: the values of the variables in the sta task loop over the iterations needed for convergence; the thermodynamic properties of the hydrogen propellant at the exit of each engine cycle component; and the key parameters, both entered into the computer and calculated, for each system component.

The key information required for this study is the maximum nozzle temperature in the final iteration, the thrust and specific impulse of the engine, and the power production/ consumption of the TPA components for each engine cycle. This information is summarized below.

For the two bleed cycles, it was assumed that the small amount of thrust produced by the gas turbine exhaust would not be useful thrust, since it would most likely not be exhausted parallel to the flight path. Therefore, the engine thrust was taken to be the thrust from the main exhaust nozzle, and the engine specific impulse was calculated as the main nozzle thrust divided by the total propellant weight flow rate.

Table 1. 2000 MW Engine for Mars Mission			
	Bleed Cycle (Uncooled Nozzle)	Bleed Cycle (Cooled Cycle)	Expander Cycle
Maximum Nozzle Temp (k)	N/A	942	950
Thrust (kn)	454	452	460
Specific Impulse (sec)	1157	1153	1175
Power (MW)			
Gas Turbine	4.44	5.47	8.15
Pump 1	–4.44	–4.44	–4.43
Pump 2	N/A	–1.02	–3.59
Balance	0.0	0.0	0.13

Table 2. 150 MW Engine for GTV Mission			
	Bleed Cycle (Uncooled Nozzle)	Bleed Cycle (Cooled Cycle)	Expander Cycle
Maximum Nozzle Temp (k)	N/A	852	856
Thrust (kn)	43.2	43.0	43.7
Specific Impulse (sec)	1159	1153	1175
Power (MW)			
Gas Turbine	0.421	0.584	1.143
Pump 1	–0.421	–0.421	–0.421
Pump 2	N/A	–0.162	–0.365
Balance	0.0	0.0	0.357

The maximum temperature reached in the aluminum nozzle for the four cooled-nozzle cycles is above the design requirement of 780 K, and in the case of the 2000 MW engine, above the melting point of the aluminum. These temperatures occur at the nozzle throat where there is the least surface area available for coolant flow. This problem could be easily solved by lining the throat area with a composite or alloy material capable of withstanding the maximum temperatures calculated. This technique is currently used in chemical rocket engine nozzles. Other than at the throat, the aluminum nozzles for both the bleed and expander cycles can be sufficiently cooled.

The TPA power balance for the bleed cycles was accomplished in the programming. For the expander cycle, the program had difficulty converging, so the necessary parameters were varied manually. As can be seen in the previous mission tables, the actual power produced by the gas turbine exceeded pump requirements. The power requirements for an actual system would probably differ slightly since very basic performance maps of the TPA components were used. However, the turbine and pump efficiencies, which are the key performance parameters, were conservatively assumed to be 80% and 70%, respectively, for a total TPA efficiency of 56%. This study indicates, contrary to some previous analyses, that the expander cycle can in fact be used with a high pressure (60 atm) PBR. The key difference between this study and the previous analyses appears to be the inclusion of nuclear heating effects in the aluminum nozzle. With this added energy the temperature of the propellant exiting the cooling jacket is much higher (467 K for the 150 MW PBR) than the temperature predicted by BNL (90 K [Ref, 4, 71]), thus giving the propellant the necessary enthalpy to operate the TPA.

The choice of which engine cycle to use should not be based strictly on the specific impulse, but rather on the effect the specific impulse has on the initial system mass and the payload mass in conjunction with other considerations. For a possible manned mission to Mars, engine cycle comparisons should be based on returning equal payloads to earth orbit. The different specific impulses, then, affect the initial mass in earth orbit (IMEO) required for the mission according to the formula:

$$\delta V = (I_{sp}) (g_0) (ln[MR]) \qquad\qquad 6.$$

Table 2. 150 MW Engine for OTV Mission			
	Bleed Cycle (Uncooled Nozzle)	Bleed Cycle (Cooled Cycle)	Expander Cycle
Maximum Nozzle Temp (k)	N/A	852	856
Thrust (kn)	43.2	43.0	43.7
Specific Impulse (sec)	1159	1153	1175
Power (MW)			
Gas Turbine	0.421	0.584	1.143
Pump 1	-0.421	-0.421	-0.421
Pump 2	N/A	-0.162	-0.365
Balance	0.0	0.0	0.357

The maximum temperature reached in the aluminum nozzle for the four cooled-nozzle cycles is above the design requirement of 780 K, and in the case of the 2000 MW engine, above the melting point of the aluminum. These temperatures occur at the nozzle throat where there is the least surface area available for coolant flow. This problem could be easily solved by lining the throat area with a composite or alloy material capable of withstanding the maximum temperatures calculated. This technique is currently used in chemical rocket engine nozzles. Other than at the throat, the aluminum nozzles for both the bleed and expander cycles can be sufficiently cooled.

The TPA power balance for the bleed cycles was accomplished in the programming. For the expander cycle, the program had difficulty converging, so the necessary parameters were varied manually. As can be seen in the previous mission tables, the actual power produced by the gas turbine exceeded pump requirements. The power requirements for an actual system would probably differ slightly since very basic performance maps of the TPA components were used. However, the turbine and pump efficiencies, which are the key performance parameters, were conservatively assumed to be 80% and 70%, respectively, for a total TPA efficiency of 56%. This study indicates, contrary to some previous analyses, that the expander cycle can in fact be used with a high pressure (60 atm) PBR. The key difference between this study and the previous analyses appears to be the inclusion of nuclear heating effects in the aluminum nozzle. With this added energy the temperature of the propellant exiting the cooling jacket is much higher (467 K for the 150 MW PBR) than the temperature predicted by BNL (90 K [Ref. 4, 71]), thus giving the propellant the necessary enthalpy to operate the TPA.

The choice of which engine cycle to use should not be based strictly on the specific impulse, but rather on the effect the specific impulse has on the initial system mass and the payload mass in conjunction with other considerations. For a possible manned mission to Mars, engine cycle comparisons should be based on returning equal payloads to earth orbit. The different specific impulses, then, affect the initial mass in earth orbit (IMEO) required for the mission according to the formula:

$$\delta V = (I_{sp})(g_0)(\ln[MR])$$
6.

where MR is the ratio of IMEO to the payload mass and a single stage rocket is assumed. For a delta V requirement of 60000 ft/sec for a Mars mission, the results are shown below (see Appendix O).

Table 3. Mars Mission			
	Bleed Cycle (Uncooled Cycle)	Bleed Cycle (Cooled Cycle	Expander Cycle
Normalized IMEO for Equal Payload Mass	1.027	1.034	1.0

This information is based on equal payload masses, which includes the weight of the engine. For the two cooled-nozzle cycles, the engine weight includes a regeneratively cooled aluminum nozzle which is heavier than a carbon-carbon nozzle, thus reducing the useful payload weight. In addition, these cycles require a second turbopump. For the expander cycle, the gas turbine will also be larger because it must handle a greater mass flow rate. This extra engine weight should be a much smaller percentage of the total payload weight than the percentage difference among the initial masses due to the improved specific impulse. The expander cycle should still minimize IMEO for equal useful payload weight returned to earth. Therefore, it appears that an expander cycle with a cooled aluminum nozzle is the best cycle to pursue for a possible manned mission to Mars.

For a LEO to GEO OTV mission, the engine cycles should be compared based on equal initial masses since the initial mass is constrained by the launch vehicle. Assuming a single stage rocket and a delta V requirement of 14000 ft/sec, the results are:

Table 4. OTV Mission			
	Bleed Cycle (Uncooled Cycle)	Bleed Cycle (Cooled Cycle	Expander Cycle
Normalized Payload Mass for Equal Initial Mass	0.995	0.993	1.0

For this mission, since the delta V requirement is much smaller, the effect of the different specific impulses is not as significant. While the expander cycle can place more mass into GEO, this mass includes the mass of the heavier aluminum nozzle, the second turbopump, and the larger gas turbine. This extra mass is likely to account for more than 0.5% of the total payload mass. Therefore, the bleed cycle with an uncooled carbon-carbon nozzle would maximize the useful payload placed in GEO. The choice of this cycle, though, is dependent on the successful demonstration that a carbon-carbon nozzle can operate at a temperature of 3000 K. If an uncooled carbon-carbon nozzle is not feasible, the expander cycle would maximize the useful payload weight as long as the extra weight of the larger gas turbine is less than 0.7% of the total payload weight; otherwise, the bleed cycle would maximize useful payload weight.

RECOMMENDATIONS AND CONCLUSIONS

This study indicates that a regeneratively cooled aluminum nozzle can be sufficiently cooled to allow its use with a PBR rocket engine. This result is based on nozzle heating due to hot exhaust gases at a maximum chamber temperature and nuclear heating effects. The highest temperatures occur at the nozzle throat, where a composite or alloy coating could protect the aluminum. Further investigation of nozzle cooling should include modeling the nozzle with more nodes, and including more accurate dimensions for the nozzle wall thicknesses and coolant flow passages.

The study also indicates that an expander cycle with a cooled aluminum nozzle can operate with a high pressure PBR at realistic TPA efficiencies. Further investigation should include the improvements to the regeneratively cooled nozzle model and more accurate performance maps for the TPA components.

The system modeling conducted in this study at steady-state indicates that for a possible manned mission to Mars an expander cycle with a cooled aluminum nozzle would minimize the initial mass in earth orbit required for the mission, and that for a LEO to GEO orbital transfer vehicle a hot gas bleed cycle with an uncooled carbon-carbon nozzle would maximize the useful payload delivered to geosynchronous equatorial orbit. Further analyses of engine cycles should include transient modeling of the cycles and a better model for the Particle Bed Reactor. Transient analysis may indicate other considerations, such as start-up time or failure modes, which may affect the engine cycle choice.

ACKNOWLEDGMENTS

LIST OF REFERENCES

[1] George P. Sutton, Rocket Propulsion Elements, *John Wiley & Sons*, 5th. Ed., 1986.

[2] Timothy J. Lawrence and Ralph J. Cerbone, "High Energy Propulsion Systems Engine Cycle Analysis", to be published in the Proceedings of the AIAA Joint Propulsion Conference,Orlando, Florida, 15 July 1990.

[3] Private Communication with David R. Perkins, Astronautics Laboratory.

[4] J.R. Powell, et.al., "Particle Bed Reactor Orbital Transfer Vehicle Concept", AFAL-TR-88-014, July 1988.

[5] Private Communication with Dr. Ralph J. Cerbone, Brookhaven National Laboratory.

[6] Howard Geyer, "C++ Version of SALT", Argonne National Laboratory Technical Report, October 1989.

[7] Charles E. Taylor, "Expanded Liquid Engine Simulation (ELES) Computer Program Technical Information Manual", AeroJet TechSystems Company, August 1984.

[8] Charles R. King, "Compilation of Thermodynamic Properties, Transport Properties, and Theoretical Rocket Performance of Gaseous Hydrogen", National Aeronautics and Space Administration, Lewis Research Center, 1960.

[9] R.V. ʾatch, "Thermodynamic Properties and Theoretical Rocket, Performance of Hydrogen to 100000 K and 1.01325x108 N/m2", NASA, Lewis Research Center, 1971.

[10] R.L. Miller, "Heating Rates in a High Energy Propulsion, System (HEPS) Orbital Transfer Vehicle (OTV)", AL-TR-89-056, October 1989.

```
/* REGENERATIVELY COOLED NOZZLE MODEL
   written by: Cadet David E. Suzuki
               United States Air Force Academy
         for: Advanced Concepts Branch
               Astronautical Sciences Division
               Astronautics Laboratory
          on: 13 June 1990

   This model simulates the heating of a fluid in the cooling jacket
   of a regeneratively cooled nozzle.  Nozzle heating due to exhaust gases
   and nuclear heating are considered.  The model requires the following
   inputs:

       cpres       constant pressure specific heat of fluid (kJ/kg-K)
       gamm        ratio of specific heats, Cp/Cv
       k           thermal conductivity of nozzle wall (kW/m-K)
       lw          thickness of nozzle wall (m)
       maxtc       maximum design chamber temperature (K)
       twmax       maximum allowable nozzle wall temperature (K)
       tc          initial guess of chamber temperature (K)
       hg[i]       hot gas side film coefficient for the ith node (kW/m2-K)
       ar[i]       area ratio of the nozzle at the ith node
       surf[i]     surface area available for heat transfer at the ith node (m2)
       rat_m       rated/design point mass flow (kg/s)
       rat_pf      rated/design point pressure drop (fraction of inlet pressure)
       q_nuc       heat due to nuclear heating to be removed (kW/m2)
       hlmax       maximum achievable coolant side film coefficient (kW/m2-K)
       stat        turns on (=1) or off (=0) steady state option

   This model requires an externally imposed variable and constraint so
   that the assumed chamber temperature will match the actual chamber
   temperature.  The required code is:

       vary (rgen.tc, rgen.tc, min, max);


       ...
           rgen(); ... chamber(); ... nozzle();
                                              ...

       cons (rgen.tc, chamber.fl.t-rgen.tc);

     where chamber is the combustor, reactor, or other heating source.
*/


rgen::rgen(char *c)
    {strcpy(name,c); namp=name;
     cpres=14.3214; gamm=1.404; maxtc=3400.0;
     twmax=780.; k=.23; tc=2000.; lw=0.0025;
     rat_pf=.20; rat_m=15.0; q_nuc=1000.; hlmax=220.; stat=0;
     mods.put(this);
     }

void rgen::c()
    {double hl[12], tcw, tb, q, delt, dp, pr, tgas, maxwt, hl2, maxwt2;
     int i;
     fl=*gasget(); fl.namp=name;
     if (stat) rat_m=fl.m;

     // determine needed coolant side film coefficients at max design temperature
     if (dyn.state==0 || stat)
       {tb=fl.t;
        for (i=0; i<12; i++)
        // repeat for the number of nodes chosen
           {pr=exp( (log(ar[i])/.80065) -
             .87203*exp( 1.56518-pow( ((ar[i]-1)*1.11252),.43032 ) ) );
```

```
            if (i<9) tgas=maxtc*pow( (1./pr),((gamm-1.)/gamm) );
               //nodes below throat
            else tgas=maxtc;
               // nodes at throat and above
            if (tgas>=twmax)
              q=hg[i]*(tgas-twmax);
            else q=0.00001;
            tcw=twmax-q*lw/k;
            hl[i]=q/(tcw-tb);
            hl2=q_nuc/(twmax-tb);
            if (hl2>hl[i])
               {hl[i]=hl2;
                q=(tgas-tb)/(1./hg[i]+lw/k+1./hl[i]);
               }
            if (hl[i]<0. || hl[i]>hlmax)
            // change max wall temperature for unreasonable values of film coefficient
               {maxwt=twmax;
                a.prt=0; a.maxit=15;
                while (a())
                   {vary (maxwt, ((twmax+tgas)/2.), twmax, tgas);
                    q=hg[i]*(tgas-maxwt);
                    tcw=maxwt-q*lw/k;
                    hl[i]=q/(tcw-tb);
                    cons (maxwt, hl[i]-hlmax);
                   }
                maxwt2=q_nuc/hl[i]+tb;
                printf("\n\n ***WARNING: Design nozzle temp at section %.2d is \n",i);
                printf("                    Exhaust side= %.4e  Space side= %.4e \n",
                   maxwt,maxwt2);
               }
            delt=(q+q_nuc)*surf[i]/cpres/rat_m;
            tb+=delt;
           }
       }

    // calculate actual temperature rise of fluid
    tb=fl.t;
    for (i=0; i<12; i++)
      {pr=exp( (log(ar[i]))/.80065) -
         .87203*exp( 1.56518-pow( ((ar[i]-1)*1.11252),.43032 ) ) );
       if (i<9) tgas=tc*pow( (1./pr),((gamm-1.)/gamm) );
       else tgas=tc;
       q=(tgas-tb)/ 1./(hg[i]*pow((fl.m/rat_m),0.8))+lw/k+
         1./(hl[i]*pow((fl.m/rat_m),0.8)));
       delt=(q+q_nuc)*surf[i]/cpres/fl.m;
       tb+=delt;
      }

    // calculate other fluid properties
    fl.t=tb;
    dp=rat_pf*fl.p*(fl.m/rat_m)*(fl.m/rat_m);
    fl.p-=dp;
    fl.prop('t');
    fl.put();
   }

void rgen::print(void *c)
   {if (c==0) return;
    printf("\n%-12s tcomb=%.4e rat_m=%.4e",name,tc,rat_m);
   }
```

```c
/* Bleed Cycle with 2000 MW PBR and uncooled nozzle
   written by: Cadet David E. Suzuki
               United States Air Force Academy
          for: Advanced Concepts Branch
               Astronautical Sciences Division
               Astronautics Laboratory
           on: 22 June 1990
*/


#include "modd.h"
#define P 1.01325e5
task dyn="dyn", sta="sta";
stack mods,gass,shfts;

main()
  {
    gas  gas_1="gas_1";  gas_1.id="THR-tH2"; gas_1.t=20.0;
      gas_1.p=0.1e6/P;
      gas_1.m=40.;  gas_1.v=10.0;  gas_1.q=0.0;
      gas_1.diam=0.1;  gas_1.stat=1;
    valv  valv_1="valv_1";  valv_1.pf=0.01;
    pi  pi_1="pi_1";  pi_1.num=0;  pi_1.num_par=1;
      pi_1.rat_pf=0.0001;  pi_1.rat_m=40.;  pi_1.length=1.0;
      pi_1.diam=0.1;
    pump  pump_1="pump_1";  pump_1.rat_m=40.;  pump_1.rat_dp=6.0e6/P;
      pump_1.rat_eff=0.7;  pump_1.rat_rpm=60000;  pump_1.eff=0.7;
      pump_1.inertia=0.1;
    pi  pi_2="pi_2";  pi_2.num=0;  pi_2.num_par=1;
      pi_2.rat_pf=0.0001;  pi_2.rat_m=39.6;  pi_2.length=1.0;
      pi_2.diam=0.1;
    htss  htss_1="htss_1"; htss_1.temp=3000.; htss_1.pfrac=0.05;
    sp  sp_2="sp_2";  sp_2.sr=0.01;  sp_2.diam[0]=0.43;
      sp_2.diam[1]=0.1;  sp_2.stat=0;
    exnz  exnz_1="exnz_1";  exnz_1.diam=0.25;  exnz_1.eff=0.85;
      exnz_1.ratio=125.;  exnz_1.stat=1;
    valv  valv_2="valv_2";  valv_2.pf=0.1;
    pi  pi_3="pi_3";  pi_3.num=0;  pi_3.num_par=1;
      pi_3.rat_pf=0.0001;  pi_3.rat_m=0.4;  pi_3.length=1.0;
      pi_3.diam=0.01;
    mx  mx_1="mx_1";  mx_1.diam=0.1;  mx_1.stat=0;
    pi  pi_4="pi_4";  pi_4.num=0;  pi_4.num_par=1;
      pi_4.rat_pf=0.0001;  pi_4.rat_m=0.8;  pi_4.length=1.0;
      pi_4.diam=0.1;
    valv  valv_3="valv_3";  valv_3.pf=0.01;
    gt  gt_1="gt_1";  gt_1.rat_eff=0.8;  gt_1.rat_pr=10.0;
      gt_1.inertia=1.0;  gt_1.stat=1;
    exnz  exnz_2="exnz_2";  exnz_2.diam=0.05;  exnz_2.eff=0.6;
      exnz_2.ratio=1.;  exnz_2.stat=1;
    sp  sp_1="sp_1";  sp_1.sr=0.01;  sp_1.diam[0]=0.1;
      sp_1.diam[1]=0.01;  sp_1.stat=0;
    shft  shft_1="shft_1";  shft_1.rpm=60000;
    valv  valv_4="valv_4";  valv_4.pf=0.01;


    pump_1.in(); gt_1.in();

    sta.prt=2; sta.acc=1e-3;
    while (sta())
      {
        vary(valv_2.pf, valv_2.pf, .02, .17);

        gas_1();    valv_1();    pi_1();
        shft_1();    pump_1();    sp_1();    pi_2();
        htss_1();    sp_2();    exnz_1();    sp_1.s();
```

```
        valv_2();    pi_3();    mx_1.s();    sp_2.s();
        valv_4();    mx_1();    pi_4();    valv_3();
        gt_1();    exnz_2(); shft_1.end();

        cons(sp_1.sr, pi_4.fl.t-1300.);
        cons(sp_2.sr, gt_1.power+pump_1.power);
    }

 gass.print();  mods.print();
}
```

```
/* Bleed Cycle with 150 MW PBR and uncooled nozzle
   written by: Cadet David E. Suzuki
               United States Air Force Academy
           for: Advanced Concepts Branch
               Astronautical Sciences Division
               Astronautics Laboratory
           on: 22 June 1990
*/


#include "modd.h"
#define P 1.01325e5
task dyn="dyn", sta="sta";
stack mods,gass,shfts;

main()
  {
   gas  gas_1="gas_1";  gas_1.id="THR-tH2"; gas_1.t=20.0;
     gas_1.p=0.1e6/P;
     gas_1.m=3.8;  gas_1.v=10.0;  gas_1.q=0.0;
     gas_1.diam=0.05;  gas_1.stat=1;
   valv  valv_1="valv_1";  valv_1.pf=0.1;
   pi  pi_1="pi_1";  pi_1.num=0;  pi_1.num_par=1;
     pi_1.rat_pf=0.0001;  pi_1.rat_m=3.8;  pi_1.length=1.0;
     pi_1.diam=0.05;
   pump  pump_1="pump_1";  pump_1.rat_m=3.8;  pump_1.rat_dp=6.0e6/P;
     pump_1.rat_eff=0.7;  pump_1.rat_rpm=30000;  pump_1.eff=0.7;
     pump_1.inertia=0.1;
   pi  pi_2="pi_2";  pi_2.num=0;  pi_2.num_par=1;
     pi_2.rat_pf=0.0001;  pi_2.rat_m=3.8;  pi_2.length=1.0;
     pi_2.diam=0.05;
   htss  htss_1="htss_1"; htss_1.temp=3000.; htss_1.pfrac=0.05;
   sp  sp_2="sp_2";  sp_2.sr=0.01;  sp_2.diam[0]=0.11;
     sp_2.diam[1]=0.05;  sp_2.stat=0;
   exnz  exnz_1="exnz_1";  exnz_1.diam=0.05;  exnz_1.eff=0.85;
     exnz_1.ratio=125.;  exnz_1.stat=1;
   valv  valv_2="valv_2";  valv_2.pf=0.1;
   pi  pi_3="pi_3";  pi_3.num=0;  pi_3.num_par=1;
     pi_3.rat_pf=0.0001;  pi_3.rat_m=0.04;  pi_3.length=1.0;
     pi_3.diam=0.005;
   mx  mx_1="mx_1";  mx_1.diam=0.05;  mx_1.stat=0;
   pi  pi_4="pi_4";  pi_4.num=0;  pi_4.num_par=1;
     pi_4.rat_pf=0.0001;  pi_4.rat_m=0.08;  pi_4.length=1.0;
     pi_4.diam=0.05;
   valv  valv_3="valv_3";  valv_3.pf=0.1;
   gt  gt_1="gt_1";  gt_1.rat_eff=0.8;  gt_1.rat_pr=10.0;
     gt_1.inertia=1.0;  gt_1.stat=1;
   exnz  exnz_2="exnz_2";  exnz_2.diam=0.05;  exnz_2.eff=0.6;
     exnz_2.ratio=1.;  exnz_2.stat=1;
   sp  sp_1="sp_1";  sp_1.sr=0.1;  sp_1.diam[0]=0.05;
     sp_1.diam[1]=0.005;  sp_1.stat=0;
   shft  shft_1="shft_1";  shft_1.rpm=30000;
   valv  valv_4="valv_4";  valv_4.pf=0.1;


   pump_1.in(); gt_1.in();


   sta.prt=2; sta.acc=1e-3;
   while (sta())
      {
       vary(valv_2.pf, valv_2.pf, .02, .17);

       gas_1();   valv_1();   pi_1();
       shft_1();   pump_1();   sp_1();   pi_2();
       htss_1();   sp_2();   exnz_1();   sp_1.s();
```

```
    valv_2();    pi_3();    mx_1.s();    sp_2.s();
    valv_4();    mx_1();    pi_4();    valv_3();
    gt_1();    exnz_2(); shft_1.end();

    cons(sp_1.sr, pi_4.fl.t-1300.);
    cons(sp_2.sr, gt_1.power+pump_1.power);
    }

 gass.print();  mods.print();
}
```

```
/* Bleed Cycle with 2000 MW PBR and cooled nozzle
   written by: Cadet David E. Suzuki
               United States Air Force Academy
           for: Advanced Concepts Branch
               Astronautical Sciences Division
               Astronautics Laboratory
            on: 22 June 1990
*/


#include "modd.h"
#define P 1.01325e5
task dyn="dyn", sta="sta";
stack mods,gass,shfts;

main()
  {
    gas  gas_1="gas_1";  gas_1.id="THR-tH2"; gas_1.t=20.0;
      gas_1.p=0.1e6/P;
      gas_1.m=40.;  gas_1.v=10.0;  gas_1.q=0.0;
      gas_1.diam=0.1;  gas_1.stat=1;
    valv  valv_1="valv_1";  valv_1.pf=0.01;
    pi  pi_1="pi_1";  pi_1.num=0;  pi_1.num_par=1;
      pi_1.rat_pf=0.0001;  pi_1.rat_m=40.;  pi_1.length=1.0;
      pi_1.diam=0.1;
    pump  pump_1="pump_1";  pump_1.rat_m=40.;  pump_1.rat_dp=6.e6/P;
      pump_1.rat_eff=0.7;  pump_1.rat_rpm=60000;  pump_1.eff=0.7;
      pump_1.inertia=0.1;
    pi  pi_2="pi_2";  pi_2.num=0;  pi_2.num_par=1;
      pi_2.rat_pf=0.0001;  pi_2.rat_m=39.6;  pi_2.length=1.0;
      pi_2.diam=0.1;
    rgen  rgen_1="rgen_1";  rgen_1.tc=3000;  rgen_1.twmax=780.;
      rgen_1.q_nuc=1250.;  rgen_1.hlmax=225.;  rgen_1.lw=.0025;
      rgen_1.rat_pf=0.4;  rgen_1.stat=1;
//The following nozzle data is from AFAL-TR-88-014 fig 37&38
      rgen_1.hg[0]=.18;  rgen_1.ar[0]=125.;  rgen_1.surf[0]=2.6;
      rgen_1.hg[1]=.21;  rgen_1.ar[1]=112.;  rgen_1.surf[1]=2.4;
      rgen_1.hg[2]=.24;  rgen_1.ar[2]=100.;  rgen_1.surf[2]=2.3;
      rgen_1.hg[3]=.28;  rgen_1.ar[3]=83.;   rgen_1.surf[3]=2.1;
      rgen_1.hg[4]=.35;  rgen_1.ar[4]=67.;   rgen_1.surf[4]=1.9;
      rgen_1.hg[5]=.45;  rgen_1.ar[5]=53.;   rgen_1.surf[5]=1.7;
      rgen_1.hg[6]=.71;  rgen_1.ar[6]=37.;   rgen_1.surf[6]=1.4;
      rgen_1.hg[7]=1.3;  rgen_1.ar[7]=22.;   rgen_1.surf[7]=1.1;
      rgen_1.hg[8]=4.2;  rgen_1.ar[8]=9.2;   rgen_1.surf[8]=.69;
      rgen_1.hg[9]=20.;  rgen_1.ar[9]=1.0;   rgen_1.surf[9]=.23;
      rgen_1.hg[10]=1.8; rgen_1.ar[10]=27.;  rgen_1.surf[10]=1.2;
      rgen_1.hg[11]=.63; rgen_1.ar[11]=67.;  rgen_1.surf[11]=1.9;
    htss  htss_1="htss_1"; htss_1.temp=3000.; htss_1.pfrac=0.05;
    sp  sp_2="sp_2";  sp_2.sr=0.01;  sp_2.diam[0]=0.43;
      sp_2.diam[1]=0.1;  sp_2.stat=0;
    exnz  exnz_1="exnz_1";  exnz_1.diam=0.25;  exnz_1.eff=0.85;
      exnz_1.ratio=125.;  exnz_1.stat=1;
    valv  valv_2="valv_2";  valv_2.pf=0.1;
    pi  pi_3="pi_3";  pi_3.num=0;  pi_3.num_par=1;
      pi_3.rat_pf=0.0001;  pi_3.rat_m=0.4;  pi_3.length=1.0;
      pi_3.diam=0.01;
    mx  mx_1="mx_1";  mx_1.diam=0.1;  mx_1.stat=0;
    pi  pi_4="pi_4";  pi_4.num=0;  pi_4.num_par=1;
      pi_4.rat_pf=0.0001;  pi_4.rat_m=0.8;  pi_4.length=1.0;
      pi_4.diam=0.1;
    valv  valv_3="valv_3";  valv_3.pf=0.01;
    gt  gt_1="gt_1";  gt_1.rat_eff=0.8;  gt_1.rat_pr=10.0;
      gt_1.inertia=1.0;  gt_1.stat=1;
    exnz  exnz_2="exnz_2";  exnz_2.diam=0.05;  exnz_2.eff=0.6;
```

```
    exnz_2.ratio=1.;   exnz_2.stat=1;
sp  sp_1="sp_1";   sp_1.sr=0.01;   sp_1.diam[0]=0.1;
  sp_1.diam[1]=0.01;   sp_1.stat=0;
shft  shft_1="shft_1";   shft_1.rpm=60000;
valv  valv_4="valv_4";   valv_4.pf=0.01;
sp  sp_3="sp_3";   sp_3.sr=0.7;   sp_3.diam[0]=0.1;
  sp_3.diam[1]=0.01;   sp_3.stat=1;
pump  pump_2="pump_2";   pump_2.rat_m=12.;   pump_2.rat_dp=4.e6/P;
  pump_2.rat_eff=0.7;   pump_2.rat_rpm=60000;   pump_2.eff=0.7;
  pump_2.inertia=0.1;
mx  mx_2="mx_2";   mx_2.diam=0.1;   mx_2.stat=0;
valv  valv_5="valv_5";   valv_5.pf=0.1;

pump_1.in();   pump_2.in();   gt_1.in();

sta.prt=2;  sta.acc=1e-3;
while (sta())
   {
    vary(valv_2.pf, valv_2.pf, .02, .17);
    vary(valv_5.pf, valv_5.pf, .001, .17);

    gas_1();    valv_1();    pi_1();
    shft_1();   pump_1();   sp_3();   pump_2();
    pi_2();   rgen_1();   sp_1();   mx_2.s();   sp_3.s();   valv_5();
    mx_2();   htss_1();   sp_2();   exnz_1();   sp_1.s();
    valv_2();   pi_3();   mx_1.s();   sp_2.s();
    valv_4();   mx_1();   pi_4();   valv_3();
    gt_1();   exnz_2();

    cons(sp_1.sr, pi_4.fl.t-1300.);
    cons(sp_2.sr, gt_1.power+pump_1.power+pump_2.power);
   }

 gass.print();   mods.print();
}
```

```
/* Bleed Cycle with 150 MW PBR and cooled nozzle
    written by: Cadet David E. Suzuki
                United States Air Force Academy
          for: Advanced Concepts Branch
                Astronautical Sciences Division
                Astronautics Laboratory
            on: 22 June 1990
*/


#include "modd.h"
#define P 1.01325e5
task dyn="dyn", sta="sta";
stack mods,gass,shfts;


main()
  {
    gas gas_1="gas_1"; gas_1.id="THR-tH2"; gas_1.t=20.0;
      gas_1.p=0.1e6/P;
      gas_1.m=3.8; gas_1.v=10.0; gas_1.q=0.0;
      gas_1.diam=0.05; gas_1.stat=1;
    valv valv_1="valv_1"; valv_1.pf=0.1;
    pi pi_1="pi_1"; pi_1.num=0; pi_1.num_par=1;
      pi_1.rat_pf=0.0001; pi_1.rat_m=3.8; pi_1.length=1.0;
      pi_1.diam=0.05;
    pump pump_1="pump_1"; pump_1.rat_m=3.8; pump_1.rat_dp=6.e6/P;
      pump_1.rat_eff=0.7; pump_1.rat_rpm=30000; pump_1.eff=0.7;
      pump_1.inertia=0.1;
    pi pi_2="pi_2"; pi_2.num=0; pi_2.num_par=1;
      pi_2.rat_pf=0.0001; pi_2.rat_m=3.8; pi_2.length=1.0;
      pi_2.diam=0.05;
    rgen rgen_1="rgen_1"; rgen_1.tc=3000; rgen_1.twmax=780.;
      rgen_1.q_nuc=93.; rgen_1.hlmax=225.; rgen_1.lw=.0025;
      rgen_1.rat_pf=0.4; rgen_1.stat=1;
//The following nozzle data is from AFAL-TR-88-014 fig 37&38
      rgen_1.hg[0]=.18; rgen_1.ar[0]=125.; rgen_1.surf[0]=.17;
      rgen_1.hg[1]=.21; rgen_1.ar[1]=112.; rgen_1.surf[1]=.11;
      rgen_1.hg[2]=.24; rgen_1.ar[2]=100.; rgen_1.surf[2]=.021;
      rgen_1.hg[3]=.28; rgen_1.ar[3]=83.; rgen_1.surf[3]=.063;
      rgen_1.hg[4]=.35; rgen_1.ar[4]=67.; rgen_1.surf[4]=.097;
      rgen_1.hg[5]=.45; rgen_1.ar[5]=53.; rgen_1.surf[5]=.13;
      rgen_1.hg[6]=.71; rgen_1.ar[6]=37.; rgen_1.surf[6]=.15;
      rgen_1.hg[7]=1.3; rgen_1.ar[7]=22.; rgen_1.surf[7]=.17;
      rgen_1.hg[8]=4.2; rgen_1.ar[8]=9.2; rgen_1.surf[8]=.19;
      rgen_1.hg[9]=20.; rgen_1.ar[9]=1.0; rgen_1.surf[9]=.21;
      rgen_1.hg[10]=1.8; rgen_1.ar[10]=27.; rgen_1.surf[10]=.22;
      rgen_1.hg[11]=.63; rgen_1.ar[11]=67.; rgen_1.surf[11]=.23;
    htss htss_1="htss_1"; htss_1.temp=3000.; htss_1.pfrac=0.05;
    sp sp_2="sp_2"; sp_2.sr=0.01; sp_2.diam[0]=0.11;
      sp_2.diam[1]=0.05; sp_2.stat 0;
    exnz exnz_1="exnz_1"; exnz_1.diam=0.05; exnz_1.eff=0.85;
      exnz_1.ratio=125.; exnz_1.stat=1;
    valv valv_2="valv_2"; valv_2.pf=0.1;
    pi pi_3="pi_3"; pi_3.num=0; pi_3.num_par=1;
      pi_3.rat_pf=0.0001; pi_3.rat_m=0.04; pi_3.length=1.0;
      pi_3.diam=0.005;
    mx mx_1="mx_1"; mx_1.diam=0.05; mx_1.stat=0;
    pi pi_4="pi_4"; pi_4.num=0; pi_4.num_par=1;
      pi_4.rat_pf=0.0001; pi_4.rat_m=0.08; pi_4.length=1.0;
      pi_4.diam=0.05;
    valv valv_3="valv_3"; valv_3.pf=0.1;
    gt gt_1="gt_1"; gt_1.rat_eff=0.8; gt_1.rat_pr=10.0;
      gt_1.inertia=1.0; gt_1.stat=1;
    exnz exnz_2="exnz_2"; exnz_2.diam=0.05; exnz_2.eff=0.6;
```

```
    exnz_2.ratio=1.;   exnz_2.stat=1;
sp  sp_1="sp_1";   sp_1.sr=0.1;   sp_1.diam[0]=0.05;
   sp_1.diam[1]=0.005;   sp_1.stat=0;
shft  shft_1="shft_1";   shft_1.rpm=30000;
valv  valv_4="valv_4";   valv_4.pf=0.1;
sp  sp_3="sp_3";   sp_3.sr=0.5;   sp_3.diam[0]=0.05;
   sp_3.diam[1]=0.005;   sp_3.stat=1;
pump  pump_2="pump_2";   pump_2.rat_m=1.9;   pump_2.rat_dp=4.e6/P;
   pump_2.rat_eff=0.7;   pump_2.rat_rpm=30000;   pump_2.eff=0.7;
   pump_2.inertia=0.1;
mx  mx_2="mx_2";   mx_2.diam=0.05;   mx_2.stat=0;
valv  valv_5="valv_5";   valv_5.pf=0.1;

pump_1.in();   pump_2.in();   gt_1.in();

sta.prt=2; sta.acc=1e-3;
while (sta())
    {
    vary(valv_2.pf, valv_2.pf, .02, .17);
    vary(valv_5.pf, valv_5.pf, .001, .17);

    gas_1();    valv_1();    pi_1();
    shft_1();    pump_1();   sp_3();   pump_2();
    pi_2();   rgen_1();   sp_1();    mx_2.s();   sp_3.s();   valv_5();
    mx_2();   htss_1();    sp_2();    exnz_1();    sp_1.s();
    valv_2();    pi_3();    mx_1.s();    sp_2.s();
    valv_4();    mx_1();    pi_4();    valv_3();
    gt_1();    exnz_2();

    cons(sp_1.sr, pi_4.fl.t-1300.);
    cons(sp_2.sr, gt_1.power+pump_1.power+pump_2.power);
    }

gass.print();   mods.print();
}
```

assume H_2 at ~100 K, ~100 atm.

constrain max. coolant velocity to Mach 0.2

*H_2 properties are taken from Ref 8 and Ref 9

$$a = \sqrt{\gamma RT} = \sqrt{(1.8)(8.314 \frac{KJ}{Kg \cdot K})(100 K)}$$

$$a = 1223 \; m/sec$$

$$V = .2 \cdot a = 245 \; m/sec$$

use continuity to find flow area

$$\dot{m} = \rho V A$$

$$A = \dot{m}/\rho V = \frac{40 \; Kg/s}{7 \frac{Kg}{m^3} \cdot 245 \frac{m}{sec}} = .0232 \; m^2$$

for a .23 m diameter throat, the channel thickness is approx.

$$t \cong \frac{.0232 m^2}{\pi \cdot .23 m} = .032 \; m = 3.2 \; cm$$

which is unreasonable

set $\dot{m}$ at 30% of flow = 12 Kg/sec

so $t \cong .96 \; cm$

assume 50 circular channels

$$\dot{m} = \frac{12}{50} = .24 \; Kg/sec \quad \text{mass flow}$$

$$D \cong \frac{\pi \cdot .23 \, m}{50} = .0145 m \quad \text{diameter}$$

} for each coolant channel

for H_2

$$Nu = (.208) \left(\frac{Re}{\mu}\right)^{.8} (Pr)^{.4} \qquad (Ref \; 7, \; p37)$$

$$Nu = hD/k$$

$$Re = \rho DV = \rho DV \cdot \frac{\frac{\pi}{4}}{\frac{\pi}{4}} = \frac{4\rho VA}{D\pi} = \frac{4\dot{m}}{D\pi}$$

$$Pr = \frac{C_p \mu}{K}$$

$$\frac{hD}{k} = (.208)\left(\frac{4\dot{m}}{D\pi\mu}\right)^{.8}\left(\frac{c_p\mu}{k}\right)^{.4}$$

$$h = (.208)\left(\frac{4}{\pi}\right)^{.8}\frac{(\dot{m})^{.8}(c_p)^{.4}(K)^{.6}}{(D)^{1.8}(\mu)^{.4}}$$

$$h = \frac{(.252)(.24)^{.8}(14.3214)^{.4}(8.368\times10^{-5})^{.6}}{(.0145)^{1.8}(5\times10^{-6})^{.4}}$$

$$\frac{(Kg/s)^{.8}(KJ/_{kg}K)^{.4}(Kw/_{mK})^{.6}}{(m)^{1.8}(Kg/_{m\,sec})^{.4}}$$

$$\boxed{h \approx 225 \; KW/_{m^2}K}$$

```c
/* Expander Cycle with 2000 MW PBR
    written by: Cadet David E. Suzuki
                United States Air Force Academy
            for: Advanced Concepts Branch
                Astronautical Sciences Division
                Astronautics Laboratory
            on: 22 June 1990
*/


#include "modd.h"
#define P 1.01325e5
task dyn="dyn", sta="sta";
stack mods,gass,shfts;

main()
  {
    gas  gas_1="gas_1";  gas_1.id="THR-tH2"; gas_1.t=20.0;  gas_1.p=.1e6/P;
      gas_1.m=40.;  gas_1.v=10.0;  gas_1.q=0.0;
      gas_1.diam=0.1;  gas_1.stat=1;
    valv  valv_1="valv_1";  valv_1.pf=0.1;
    pi  pi_1="pi_1";  pi_1.num=0;  pi_1.num_par=1;
      pi_1.rat_pf=0.0001;  pi_1.rat_m=40.;  pi_1.length=1.0;
      pi_1.diam=0.1;
    pump  pump_1="pump_1";  pump_1.rat_m=40.;  pump_1.rat_dp=6.0e6/P;
      pump_1.rat_eff=0.7;  pump_1.rat_rpm=60000;  pump_1.eff=0.7;
      pump_1.inertia=0.1;
    sp  sp_1="sp_1";  sp_1.sr=0.7;  sp_1.diam[0]=0.1;
      sp_1.diam[1]=0.1;  sp_1.stat=1;
    shft  shft_1="shft_1";  shft_1.rpm=60000;
    pump  pump_2="pump_2";  pump_2.rat_m=12.0;  pump_2.rat_dp=14.0e6/P;
      pump_2.rat_eff=0.7;  pump_2.rat_rpm=60000;  pump_2.eff=0.7;
      pump_2.inertia=0.1;
    pi  pi_2="pi_2";  pi_2.num=0;  pi_2.num_par=1;
      pi_2.rat_pf=0.0001;  pi_2.rat_m=20.0;  pi_2.length=1.0;
      pi_2.diam=0.1;
    valv  valv_2="valv_2";  valv_2.pf=0.01;
    pi  pi_3="pi_3";  pi_3.num=0;  pi_3.num_par=1;
      pi_3.rat_pf=0.0001;  pi_3.rat_m=30.0;  pi_3.length=1.0;
      pi_3.diam=0.1;
    mx  mx_1="mx_1";  mx_1.diam=0.1; mx_1.stat=0;
    gt  gt_1="gt_1";  gt_1.rat_eff=0.8;  gt_1.rat_pr=2.0;
      gt_1.inertia=1.0;  gt_1.stat=1;
    valv  valv_3="valv_3";  valv_3.pf=0.01;
    valv  valv_4="valv_4";  valv_4.pf=0.01;
    pi  pi_4="pi_4";  pi_4.num=0;  pi_4.num_par=1;
      pi_4.rat_pf=0.0001;  pi_4.rat_m=20.0;  pi_4.length=1.0;
      pi_4.diam=0.1;
    pi  pi_5="pi_5";  pi_5.num=0;  pi_5.num_par=1;
      pi_5.rat_pf=0.0001;  pi_5.rat_m=20.0;  pi_5.length=1.0;
      pi_5.diam=0.1;
    htss  htss_1="htss_1"; htss_1.temp=3000.; htss_1.pfrac=0.05;
    exnz  exnz_1="exnz_1";  exnz_1.diam=0.25;  exnz_1.eff=0.85;
      exnz_1.ratio=125.0;  exnz_1.stat=1;
    rgen  rgen_1="rgen_1"; rgen_1.tc=3000; rgen_1.twmax=780.;
      rgen_1.q_nuc=1250.;  rgen_1.hlmax=225.;  rgen_1.lw=.0025;
      rgen_1.rat_pf=0.4;  rgen_1.stat=1;
//The following nozzle data is from AFAL-TR-88-014 fig 37&38
      rgen_1.hg[0]=.18;  rgen_1.ar[0]=125.;  rgen_1.surf[0]=2.6;
      rgen_1.hg[1]=.21;  rgen_1.ar[1]=112.;  rgen_1.surf[1]=2.4;
      rgen_1.hg[2]=.24;  rgen_1.ar[2]=100.;  rgen_1.surf[2]=2.3;
      rgen_1.hg[3]=.28;  rgen_1.ar[3]=83.;   rgen_1.surf[3]=2.1;
      rgen_1.hg[4]=.35;  rgen_1.ar[4]=67.;   rgen_1.surf[4]=1.9;
      rgen_1.hg[5]=.45;  rgen_1.ar[5]=53.;   rgen_1.surf[5]=1.7;
```

```
       rgen_1.hg[6]=.71;   rgen_1.ar[6]=37.;   rgen_1.surf[6]=1.4;
       rgen_1.hg[7]=1.3;   rgen_1.ar[7]=22.;   rgen_1.surf[7]=1.1;
       rgen_1.hg[8]=4.2;   rgen_1.ar[8]=9.2;   rgen_1.surf[8]=.69;
       rgen_1.hg[9]=20.;   rgen_1.ar[9]=1.0;   rgen_1.surf[9]=.23;
       rgen_1.hg[10]=1.8;  rgen_1.ar[10]=27.;  rgen_1.surf[10]=1.2;
       rgen_1.hg[11]=.63;  rgen_1.ar[11]=67.;  rgen_1.surf[11]=1.9;

   pump_1.in(); pump_2.in(); gt_1.in();

   sta.prt=2; sta.acc=1.0e-3;
   while (sta())
   {vary(valv_2.pf, valv_2.pf, 0.001, 0.4);

    vary(rgen_1.tc, rgen_1.tc, 500., 3500.);

    gas_1();    valv_1();    pi_1();
    shft_1();    pump_1();    sp_1();    pump_2();    pi_2();
    rgen_1();    pi_4();    valv_3();    gt_1();
    pi_5();   valv_4();    mx_1.s();    sp_1.s();    valv_2();
    pi_3();    mx_1();    htss_1();    exnz_1();

    cons(rgen_1.tc, htss_1.fl.t-rgen_1.tc);
   }

   gass.print();  mods.print();

   }
```

```
/* Expander Cycle with 150 MW PBR
     written by: Cadet David E. Suzuki
                 United States Air Force Academy
             for: Advanced Concepts Branch
                 Astronautical Sciences Division
                 Astronautics Laboratory
             on: 22 June 1990
*/


#include "modd.h"
#define P 1.01325e5
task dyn="dyn", sta="sta";
stack mods,gass,shfts;

main()
   {
   gas  gas_1="gas_1";  gas_1.id="THR-tH2"; gas_1.t=20.0;  gas_1.p=.1e6/P;
     gas_1.m=3.8;  gas_1.v=10.0;  gas_1.q=0.0;
     gas_1.diam=0.05;  gas_1.stat=1;
   valv  valv_1="valv_1";  valv_1.pf=0.1;
   pi  pi_1="pi_1";  pi_1.num=0;  pi_1.num_par=1;
     pi_1.rat_pf=0.0001;  pi_1.rat_m=3.8;  pi_1.length=1.0;
     pi_1.diam=0.05;
   pump  pump_1="pump_1";  pump_1.rat_m=3.8;  pump_1.rat_dp=6.0e6/P;
     pump_1.rat_eff=0.7;  pump_1.rat_rpm=30000;  pump_1.eff=0.7;
     pump_1.inertia=0.1;
   sp  sp_1="sp_1";  sp_1.sr=0.5;  sp_1.diam[0]=0.05;
     sp_1.diam[1]=0.05;  sp_1.stat=1;
   shft  shft_1="shft_1";  shft_1.rpm=30000;
   pump  pump_2="pump_2";  pump_2.rat_m=1.9;  pump_2.rat_dp=9.0e6/P;
     pump_2.rat_eff=0.7;  pump_2.rat_rpm=30000;  pump_2.eff=0.7;
     pump_2.inertia=0.1;
   pi  pi_2="pi_2";  pi_2.num=0;  pi_2.num_par=1;
     pi_2.rat_pf=0.0001;  pi_2.rat_m=1.14;  pi_2.length=1.0;
     pi_2.diam=0.05;
   valv  valv_2="valv_2";  valv_2.pf=0.01;
   pi  pi_3="pi_3";  pi_3.num=0;  pi_3.num_par=1;
     pi_3.rat_pf=0.0001;  pi_3.rat_m=2.66;  pi_3.length=1.0;
     pi_3.diam=0.05;
   mx  mx_1="mx_1";  mx_1.diam=0.05; mx_1.stat=0;
   gt  gt_1="gt_1";  gt_1.rat_eff=0.8;  gt_1.rat_pr=1.5;
     gt_1.inertia=1.0;  gt_1.stat=1;
   valv  valv_3="valv_3";  valv_3.pf=0.01;
   valv  valv_4="valv_4";  valv_4.pf=0.01;
   pi  pi_4="pi_4";  pi_4.num=0;  pi_4.num_par=1;
     pi_4.rat_pf=0.0001;  pi_4.rat_m=1.14;  pi_4.length=1.0;
     pi_4.diam=0.05;
   pi  pi_5="pi_5";  pi_5.num=0;  pi_5.num_par=1;
     pi_5.rat_pf=0.0001;  pi_5.rat_m=1.14;  pi_5.length=1.0;
     pi_5.diam=0.05;
   htss  htss_1="htss_1";  htss_1.temp=3000.;  htss_1.pfrac=0.05;
   exnz  exnz_1="exnz_1";  exnz_1.diam=0.05;  exnz_1.eff=0.85;
     exnz_1.ratio=125.0;  exnz_1.stat=1;
   rgen  rgen_1="rgen_1"; rgen_1.tc=3000; rgen_1.twmax=780.;
     rgen_1.q_nuc=93.;  rgen_1.hlmax=225.;  rgen_1.lw=.0025;
     rgen_1.rat_pf=0.4;  rgen_1.stat=1;
//The following nozzle data is from AFAL-TR-88-014 fig 37&38
     rgen_1.hg[0]=.18;  rgen_1.ar[0]=125.;  rgen_1.surf[0]=.17;
     rgen_1.hg[1]=.21;  rgen_1.ar[1]=112.;  rgen_1.surf[1]=.11;
     rgen_1.hg[2]=.24;  rgen_1.ar[2]=100.;  rgen_1.surf[2]=.021;
     rgen_1.hg[3]=.28;  rgen_1.ar[3]=83.;   rgen_1.surf[3]=.063;
     rgen_1.hg[4]=.35;  rgen_1.ar[4]=67.;   rgen_1.surf[4]=.097;
     rgen_1.hg[5]=.45;  rgen_1.ar[5]=53.;   rgen_1.surf[5]=.13;
```

H1

```
      rgen_1.hg[6]=.71;   rgen_1.ar[6]=37.;   rgen_1.surf[6]=.15;
      rgen_1.hg[7]=1.3;   rgen_1.ar[7]=22.;   rgen_1.surf[7]=.17;
      rgen_1.hg[8]=4.2;   rgen_1.ar[8]=9.2;   rgen_1.surf[8]=.19;
      rgen_1.hg[9]=20.;   rgen_1.ar[9]=1.0;   rgen_1.surf[9]=.21;
      rgen_1.hg[10]=1.8;  rgen_1.ar[10]=27.;  rgen_1.surf[10]=.22;
      rgen_1.hg[11]=.63;  rgen_1.ar[11]=67.;  rgen_1.surf[11]=.23;

pump_1.in(); pump_2.in(); gt_1.in();

sta.prt=2; sta.acc=1.0e-3;
while (sta())
{vary(valv_2.pf, valv_2.pf, 0.001, 0.4);
 vary(rgen_1.tc, rgen_1.tc, 500., 3500.);

 gas_1();    valv_1();   pi_1();
 shft_1();   pump_1();   sp_1();    pump_2();    pi_2();
 rgen_1();   pi_4();     valv_3();  gt_1();
 pi_5();   valv_4();   mx_1.s();   sp_1.s();   valv_2();
 pi_3();   mx_1();   htss_1();   exnz_1();

 cons(rgen_1.tc, htss_1.fl.t-rgen_1.tc);
 }

gass.print();  mods.print();

}
```

Bleed Cycle (Uncooled Nozzle) - 2000 MW PBR

thermodynamic data for HYDROGEN with flow id = THR-tH2
pc=12.800000, tc=33.200000, tb=20.400000, molwt=2.016000

task: sta n=0 f=2.946671e+06
  x= 1.000000e-01 1.000000e-02 1.000000e-02
  c= 2.437571e+00 3.229653e+02 2.946671e+06
  h= 1.6761e-03 hs= 1.6761e-03 mu=0.00e+00 n=1.66e-03 s=1.50e-03 a=9.92e-01

task: sta n=1 f=2.419404e+04
  x= 5.949484e-02 1.028357e-02 5.885908e-03
  c= 1.836518e-05 -8.608664e+01 -2.419389e+04
  h= 1.3500e-06 hs= 1.3500e-06 mu=0.00e+00 n=1.22e-06 s=4.49e-07 a=7.35e-01

task: sta n=2 f=7.358433e+03
  x= 5.951464e-02 9.178656e-03 5.942038e-03
  c=-2.020809e-05 3.501279e+00 7.358432e+03
  h= 2.3367e-09 hs= 2.3367e-09 mu=0.00e+00 n=1.35e-09 s=8.28e-10 a=8.43e-01

task: sta n=3 f=5.520819e+01
  x= 5.951432e-02 9.213792e-03 5.931398e-03
  c=-2.136492e-06 -6.052007e-01 -5.520487e+01
  h= 6.6674e-11 hs= 6.6674e-11 mu=0.00e+00 n=4.08e-11 s=1.87e-11 a=7.75e-01

task: sta n=4 f=1.748936e+01
  x= 5.951447e-02 9.207406e-03 5.931532e-03
  c= 1.831213e-08 -8.018754e-02 -1.748918e+01
  h= 1.1710e-12 hs= 1.1710c-12 mu=0.00c+00 n=9.23e-13 s=3.55e-13 a=7.36e-01

task: sta n=5 f=1.294911e-01
  x= 5.951449e-02 9.206446e-03 5.931569e-03
  c= 1.300933e-10 7.746009e-04 1.294888e-01
  h= 1.0924e-16 hs= 1.0924e-16 mu=0.00e+00 n=8.54e-17 s=3.29e-17 a=7.37e-01
convergence of independent variables in task sta

output of model flows

model	temp	pres	mass	enth	entr	dens	velc	qual
gas_1	20.0	0.99	40.000	-4.1280e+06	-1.0589e+05	7.712e+01	66.0	0.00
valv_1	20.0	0.98	40.000	-4.1280e+06	-1.0587e+05	7.714e+01	66.0	0.00
pi_1	20.0	0.98	40.000	-4.1280e+06	-1.0587e+05	7.714e+01	66.0	0.00
pump_1	32.7	60.19	40.000	-4.0169e+06	-1.0374e+05	6.692e+01	66.0	1.00
sp_1	32.7	60.19	39.632	-4.0169e+06	-1.0374e+05	6.692e+01	75.4	1.00
pi_2	32.7	60.19	39.632	-4.0169e+06	-1.0374e+05	6.692e+01	75.4	1.00
htss_1	3000.0	57.18	39.632	4.3764e+07	-2.9025e+04	4.664e-01	75.4	1.00
sp_2	3000.0	57.18	39.397	4.3764e+07	-2.9025e+04	4.664e-01	581.7	1.00
exnz_1	1089.7	0.30	39.397	1.1325e+07	-2.4291e+04	6.806e-03	8075.6	1.00
sp_1	32.7	60.19	0.368	-4.0169e+06	-1.0374e+05	6.692e+01	70.1	1.00
valv_2	32.6	56.61	0.368	-4.0169e+06	-1.0357e+05	6.612e+01	70.1	1.00
pi_3	32.6	56.61	0.368	-4.0169e+06	-1.0356e+05	6.612e+01	70.9	1.00
sp_2	3000.0	57.18	0.235	4.3764e+07	-2.9025e+04	4.664e-01	64.2	1.00
valv_4	3000.0	56.61	0.235	4.3764e+07	-2.8984e+04	4.617e-01	64.2	1.00
mx_1	1300.0	56.61	0.603	1.4600e+07	-4.3168e+04	1.061e+00	72.4	1.00
pi_4	1300.0	56.60	0.603	1.4600e+07	-4.3167e+04	1.061e+00	72.4	1.00
valv_3	1300.0	56.04	0.603	1.4600e+07	-4.3126e+04	1.050e+00	72.4	1.00
gt_1	814.5	5.60	0.603	7.2332e+06	-4.0667e+04	1.688e-01	72.4	1.00
exnz_2	678.0	2.95	0.603	5.2627e+06	-4.0667e+04	1.069e-01	1986.5	1.00

gas_1   diam=1.0000e-01 area=7.8540e-03
valv_1   dp=9.8692e-03 pf=1.0000e-02

```
pi_1            dp=9.7705e-05
                length=1.0000e+00 diam=1.0000e-01 area=7.8540e-03
                rat_pf=1.0000e-04 rat_m=4.0000e+01
                num_par=1
pump_1          rpm=6.0000e+04 dp=5.9216e+01 eff=7.0000e-01 power=-4.4446e+06
                rat_dp=5.9215e+01 rat_torque=7.0737e+02 rat_rpm=6.0000e+04
                rat_m=4.0000e+01 rat_eff=7.0000e-01 inertia=1.0000e-01
pi_2            dp=6.0289e-03
                length=1.0000e+00 diam=1.0000e-01 area=7.8540e-03
                rat_pf=1.0000e-04 rat_m=3.9600e+01
                num_par=1
htss_1          heat=1.8936e+09
sp_2            sr=5.9316e-03
                diam0=4.3000e-01 diam1=1.0000e-01 area0=1.4522e-01 area1=7.8540e-03
exnz_1          mreq=3.9397e+01 thrust=4.5409e+05 impulse=1.1761e+03
                diam=2.1276e-01 area=3.5554e-02
                aexp=4.4442e+00 eff=8.5000e-01
valv_2          dp=3.5824e+00 pf=5.9514e-02
pi_3            dp=4.7982e-03
                length=1.0000e+00 diam=1.0000e-02 area=7.8540e-05
                rat_pf=1.0000e-04 rat_m=4.0000e-01
                num_par=1
mx_1            diam=1.0000e-01 area=7.8540e-03
pi_4            dp=3.2196e-03
                length=1.0000e+00 diam=1.0000e-01 area=7.8540e-03
                rat_pf=1.0000e-04 rat_m=8.0000e-01
                num_par=1
valv_3          dp=5.6603e-01 pf=1.0000e-02
gt_1            rpm=6.0000e+04 eff=8.0000e-01 power=4.4446e+06
                rat_cmass=3.8821e-01 rat_cspeed=1.6641e+03
                rat_pr=1.0000e+01 inertia=1.0000e+00
exnz_2          mreq=6.0334e-01 thrust=2.0484e+03 impulse=3.4644e+02
                diam=6.0157e-02 area=2.8422e-03
                aexp=2.8422e-03 eff=6.0000e-01
sp_1            sr=9.2065e-03
                diam0=1.0000e-01 diam1=1.0000e-02 area0=7.8540e-03 area1=7.8540e-05
shft_1          rpm=6.0000e+04 power=1.2949e-01 inertia=1.1000e+00
valv_4          dp=5.7178e-01 pf=1.0000e-02
```

APPENDIX J

Bleed Cycle (Cooled Nozzle) - 2000 MW PBR

thermodynamic data for HYDROGEN with flow id = THR-tH2
pc=12.800000, tc=33.200000, tb=20.400000, molwt=2.016000

  ***WARNING: Design nozzle temp at section 09 is
            Exhaust side= 9.4185e+02 Space side= 1.9453e+02

task: sta n=0 f=1.925538e+06
  x= 1.000000e-01 1.000000e-01 1.000000e-02 1.000000e-02
  c=-5.627963e+00 -2.240998e-01 1.141654e+03 1.925537e+06

  ***WARNING: Design nozzle temp at section 09 is
            Exhaust side= 9.4185e+02 Space side= 1.9453e+02

  ***WARNING: Design nozzle temp at section 09 is
            Exhaust side= 9.4185e+02 Space side= 1.9453e+02

  ***WARNING: Design nozzle temp at section 09 is
            Exhaust side= 9.4185e+02 Space side= 1.9453e+02

  ***WARNING: Design nozzle temp at section 09 is
            Exhaust side= 9.4185e+02 Space side= 1.9453e+02

  h= 9.4372e-03 hs= 9.4372e-03 mu=2.08e-01 n=1.09e-02 s=5.14e-03 a=8.79e-01

  ***WARNING: Design nozzle temp at section 09 is
            Exhaust side= 9.4185e+02 Space side= 1.9453e+02

task: sta n=1 f=2.352508e+06
  x= 6.535756e-02 7.097487e-03 3.256879e-02 3.261585e-03
  c=-3.588697e-02 3.387519e-01 -2.342282e+02 -2.352508e+06
  h= 7.1844e-05 hs= 7.1844e-05 mu=0.00e+00 n=5.12e-05 s=2.71e-05 a=8.54e-01

  ***WARNING: Design nozzle temp at section 09 is
            Exhaust side= 9.4185e+02 Space side= 1.9453e+02

task: sta n=2 f=8.288539e+04
  x= 5.941308e-02 6.501288e-03 3.060407e-02 6.669967e-03
  c= 1.024958e-10 -4.566930e-04 2.400917e+02 8.288504e+04
  h= 2.9812e-05 hs= 2.9812e-05 mu=0.00e+00 n=1.77e-05 s=6.07e-06 a=6.68e-01

  ***WARNING: Design nozzle temp at section 09 is
            Exhaust side= 9.4185e+02 Space side= 1.9453e+02

task: sta n=3 f=1.516546e+04
  x= 5.941214e-02 6.501288e-03 3.480098e-02 6.402262e-03
  c= 9.602985e-11 8.767530e-04 1.287226e+02 -1.516491e+04
  h= 8.5659e-06 hs= 8.5659e-06 mu=0.00e+00 n=2.83e-05 s=1.89e-06 a=3.57e-01

  ***WARNING: Design nozzle temp at section 09 is
            Exhaust side= 9.4185e+02 Space side= 1.9453e+02

task: sta n=4 f=2.428594e+03

```
  x= 5.936820e-02  6.501288e-03   4.012179e-02   6.257691e-03
  c=-1.413980e-12  2.674562e-04   2.291044e+01  -2.428486e+03
  h= 2.7136e-07 hs= 2.7136e-07 mu=0.00e+00 n=1.33e-06 s=5.95e-08 a=2.99e-01

 ***WARNING: Design nozzle temp at section 09 is
             Exhaust side= 9.4185e+02  Space side= 1.9453e+02


task: sta  n=5  f=4.450260e+02
  x= 5.935641e-02  6.501288e-03   4.127555e-02   6.225847e-03
  c= 4.263256e-14  3.793903e-05   1.925824e+00  -4.450218e+02
  h= 1.9180e-09 hs= 1.9180e-09 mu=0.00e+00 n=1.16e-08 s=4.15e-10 a=2.74e-01

 ***WARNING: Design nozzle temp at section 09 is
             Exhaust side= 9.4185e+02  Space side= 1.9453e+02


task: sta  n=6  f=5.392201e+00
  x= 5.935503e-02  6.501288e-03   4.138301e-02   6.223242e-03
  c= 0.000000e+00  7.183304e-07   4.052167e-02  -5.392048e+00
  h= 8.4900e-13 hs= 8.4900e-13 mu=0.00e+00 n=5.25e-12 s=1.85e-13 a=2.70e-01

 ***WARNING: Design nozzle temp at section 09 is
             Exhaust side= 9.4185e+02  Space side= 1.9453e+02


task: sta  n=7  f=5.384589e-02
  x= 5.935500e-02  6.501288e-03   4.138529e-02   6.223181e-03
  c= 0.000000e+00  9.430750e-10 -1.355598e-04  -5.384572e-02
  h= 9.5054e-18 hs= 9.5054e-18 mu=0.00e+00 n=5.24e-17 s=2.16e-18 a=2.79e-01
convergence of independent variables in task sta

                    output of model flows

     model        temp   pres   mass     enth       entr       dens     velc   qual

  gas_1          20.0   0.99  40.000 -4.1280e+06 -1.0589e+05  7.712e+01   66.0  0.00
  valv_1         20.0   0.98  40.000 -4.1280e+06 -1.0587e+05  7.714e+01   66.0  0.00
  pi_1           20.0   0.98  40.000 -4.1280e+06 -1.0587e+05  7.714e+01   66.0  0.00
  pump_1         32.7  60.19  40.000 -4.0169e+06 -1.0374e+05  6.692e+01   66.0  1.00
  sp_3           32.7  60.19  12.000 -4.0169e+06 -1.0374e+05  6.692e+01   22.8  1.00
  pump_2         37.0  99.67  12.000 -3.9315e+06 -1.0234e+05  6.817e+01   22.8  1.00
  pi_2           37.0  99.67  12.000 -3.9315e+06 -1.0234e+05  6.817e+01   22.4  1.00
  rgen_1        311.2  59.80  12.000  1.6313e+05 -6.3960e+04  4.616e+00   22.4  1.00
  sp_1          311.2  59.80  11.503  1.6313e+05 -6.3960e+04  4.616e+00  317.3  1.00
  sp_3           32.7  60.19  28.000 -4.0169e+06 -1.0374e+05  6.692e+01 5327.6  1.00
  valv_5         32.7  59.80  28.000 -4.0169e+06 -1.0372e+05  6.685e+01 5327.6  1.00
  mx_2           97.8  59.80  39.503 -2.7997e+06 -8.0368e+04  1.569e+01  320.6  1.00
  htss_1       3000.0  56.81  39.503  4.3763e+07 -2.8999e+04  4.634e-01  320.6  1.00
  sp_2         3000.0  56.81  39.258  4.3763e+07 -2.8999e+04  4.634e-01  583.4  1.00
  exnz_1       1089.7   0.30  39.258  1.1325e+07 -2.4265e+04  6.763e-03 8075.7  1.00
  sp_1          311.2  59.80   0.497  1.6313e+05 -6.3960e+04  4.616e+00 1369.9  1.00
  valv_2        311.2  56.25   0.497  1.6313e+05 -6.3702e+04  4.349e+00 1369.9  1.00
  pi_3          311.2  56.24   0.497  1.6313e+05 -6.3702e+04  4.348e+00 1454.3  1.00
  sp_2         3000.0  56.81   0.246  4.3763e+07 -2.8999e+04  4.634e-01   67.5  1.00
  valv_4       3000.0  56.24   0.246  4.3763e+07 -2.8957e+04  4.588e-01   67.5  1.00
  mx_1         1300.0  56.24   0.742  1.4600e+07 -4.3141e+04  1.054e+00   89.7  1.00
  pi_4         1300.0  56.24   0.742  1.4600e+07 -4.3141e+04  1.054e+00   89.7  1.00
  valv_3       1300.0  55.68   0.742  1.4600e+07 -4.3099e+04  1.043e+00   89.7  1.00
  gt_1          814.5   5.57   0.742  7.2332e+06 -4.0640e+04  1.677e-01   89.7  1.00
  exnz_2        678.1   2.93   0.742  5.2638e+06 -4.0640e+04  1.062e-01 1986.6  1.00

  gas_1         diam=1.0000e-01 area=7.8540e-03
  valv_1        dp=9.8692e-03 pf=1.0000e-02
  pi_1          dp=9.7705e-05
                length=1.0000e+00 diam=1.0000e-01 area=7.8540e-03            J2
```

```
                        rat_pf=1.0000e-04 rat_m=4.0000e+01
                        num_par=1
        pump_1          rpm=6.0000e+04 dp=5.9216e+01 eff=7.0000e-01 power=-4.4446e+06
                        rat_dp=5.9215e+01 rat_torque=7.0737e+02 rat_rpm=6.0000e+04
                        rat_m=4.0000e+01 rat_eff=7.0000e-01 inertia=1.0000e-01
        pi_2            dp=9.1525e-04
                        length=1.0000e+00 diam=1.0000e-01 area=7.8540e-03
                        rat_pf=1.0000e-04 rat_m=3.9600e+01
                        num_par=1
        rgen_1          tcomb=3.0000e+03 rat_m=1.2000e+01
        htss_1          heat=1.8394e+09
        sp_2            sr=6.2232e-03
                        diam0=4.3000e-01 diam1=1.0000e-01 area0=1.4522e-01 area1=7.8540e-03
        exnz_1          mreq=3.9258e+01 thrust=4.5249e+05 impulse=1.1761e+03
                        diam=2.1306e-01 area=3.5654e-02
                        aexp=4.4567e+00 eff=8.5000e-01
        valv_2          dp=3.5495e+00 pf=5.9355e-02
        pi_3            dp=8.6711e-03
                        length=1.0000e+00 diam=1.0000e-02 area=7.8540e-05
                        rat_pf=1.0000e-04 rat_m=4.0000e-01
                        num_par=1
        mx_1            diam=1.0000e-01 area=7.8540e-03
        pi_4            dp=4.8444e-03
                        length=1.0000e+00 diam=1.0000e-01 area=7.8540e-03
                        rat_pf=1.0000e-04 rat_m=8.0000e-01
                        num_par=1
        valv_3          dp=5.6239e-01 pf=1.0000e-02
        gt_1            rpm=6.0000e+04 eff=8.0000e-01 power=5.4693e+06
                        rat_cmass=4.8082e-01 rat_cspeed=1.6641e+03
                        rat_pr=1.0000e+01 inertia=1.0000e+00
        exnz_2          mreq=7.4246e-01 thrust=2.5209e+03 impulse=3.4646e+02
                        diam=6.6937e-02 area=3.5190e-03
                        aexp=3.5190e-03 eff=6.0000e-01
        sp_1            sr=4.1385e-02
                        diam0=1.0000e-01 diam1=1.0000e-02 area0=7.8540e-03 area1=7.8540e-05
        shft_1          rpm=6.0000e+04 power=0.0000e+00 inertia=0.0000e+00
        valv_4          dp=5.6812e-01 pf=1.0000e-02
        sp_3            sr=7.0000e-01
                        diam0=1.0000e-01 diam1=1.0000e-02 area0=7.8540e-03 area1=7.8540e-05
        pump_2          rpm=6.0000e+04 dp=3.9477e+01 eff=7.0000e-01 power=-1.0247e+06
                        rat_dp=3.9477e+01 rat_torque=1.6309e+02 rat_rpm=6.0000e+04
                        rat_m=1.2000e+01 rat_eff=7.0000e-01 inertia=1.0000e-01
        mx_2            diam=1.0000e-01 area=7.8540e-03
        valv_5          dp=3.9133e-01 pf=6.5013e-03
```

EXPANDER CYCLE - 2000 MW PBR

thermodynamic data for HYDROGEN with flow id = THR-tH2
pc=12.800000, tc=33.200000, tb=20.400000, molwt=2.016000

  ***WARNING: Design nozzle temp at section 09 is
              Exhaust side= 9.4951e+02 Space side= 2.0452e+02

task: sta n=0 f=1.205471e+00
  x= 1.000000e-02 3.000000e+03
  c= 1.205471e+00 0.000000e+00

  ***WARNING: Design nozzle temp at section 09 is
              Exhaust side= 9.4951e+02 Space side= 2.0452e+02

  ***WARNING: Design nozzle temp at section 09 is
              Exhaust side= 9.4951e+02 Space side= 2.0452e+02

  h= 4.0233e-04 hs= 4.0233e-04 mu=0.00e+00 n=4.02e-04 s=4.02e-04 a=1.00e+00

  ***WARNING: Design nozzle temp at section 09 is
              Exhaust side= 9.4951e+02 Space side= 2.0452e+02

task: sta n=1 f=1.045657e-07
  x= 3.005813e-02 3.000000e+03
  c=-1.045657e-07 0.000000e+00

                    output of model flows

model	temp	pres	mass	enth	entr	dens	velc	qual
gas_1	20.0	0.99	40.000	-4.1280e+06	-1.0589e+05	7.712e+01	66.0	0.00
valv_1	19.9	0.89	40.000	-4.1280e+06	-1.0575e+05	7.731e+01	66.0	0.00
pi_1	19.9	0.89	40.000	-4.1280e+06	-1.0575e+05	7.731e+01	65.9	0.00
pump_1	32.6	60.10	40.000	-4.0171e+06	-1.0374e+05	6.692e+01	65.9	1.00
sp_1	32.6	60.10	12.000	-4.0171e+06	-1.0374e+05	6.692e+01	22.8	1.00
pump_2	47.2	198.27	12.000	-3.7183e+06	-9.9716e+04	7.047e+01	22.8	1.00
pi_2	47.2	198.27	12.000	-3.7183e+06	-9.9716e+04	7.047e+01	21.7	1.00
rgen_1	321.0	118.96	12.000	2.9423e+05	-6.6477e+04	8.682e+00	21.7	1.00
pi_4	321.0	118.96	12.000	2.9423e+05	-6.5476e+04	8.682e+00	176.0	1.00
valv_3	321.0	117.77	12.000	2.9423e+05	-6.6433e+04	8.600e+00	176.0	1.00
gt_1	271.0	58.88	12.000	-3.8524e+05	-6.5789e+04	5.219e+00	176.0	1.00
pi_5	271.0	58.88	12.000	-3.8524e+05	-6.5788e+04	5.219e+00	292.7	1.00
valv_4	271.0	58.29	12.000	-3.8524e+05	-6.5746e+04	5.169e+00	292.7	1.00
sp_1	32.6	60.10	28.000	-4.0171e+06	-1.0374e+05	6.692e+01	53.3	1.00
valv_2	32.6	58.30	28.000	-4.0171e+06	-1.0367e+05	6.659e+01	53.3	1.00
pi_3	32.6	58.29	28.000	-4.0171e+06	-1.0367e+05	6.659e+01	53.5	1.00
mx_1	89.3	58.29	40.000	-2.9276e+06	-8.1682e+04	1.711e+01	297.7	1.00
htss_1	3000.0	55.38	40.000	4.3762e+07	-2.8894e+04	4.517e-01	297.7	1.00
exnz_1	1086.8	0.29	40.000	1.1281e+07	-2.4159e+04	6.543e-03	8065.4	1.00

gas_1   diam=1.0000e-01 area=7.8540e-03
valv_1   dp=9.8692e-02 pf=1.0000e-01
pi_1   dp=8.8823e-05
            length=1.0000e+00 diam=1.0000e-01 area=7.8540e-03
            rat_pf=1.0000e-04 rat_m=4.0000e+01
            num_par=1
pump_1   rpm=6.0000e+04 dp=5.9216e+01 eff=7.0000e-01 power=-4.4346e+06
            rat_dp=5.9215e+01 rat_torque=7.0578e+02 rat_rpm=6.0000e+04
            rat_m=4.0000e+01 rat_eff=7.0000e-01 inertia=1.0000e-01
sp_1   sr=7.0000e-01

```
                    diam0=1.0000e-01 diam1=1.0000e-01 area0=7.8540e-03 area1=7.8540e-03
  shft_1            rpm=6.0000e+04 power=0.0000e+00 inertia=0.0000e+00
  pump_2            rpm=6.0000e+04 dp=1.3817e+02 eff=7.0000e-01 power=-3.5866e+06
                    rat_dp=1.3817e+02 rat_torque=5.7081e+02 rat_rpm=6.0000e+04
                    rat_m=1.2000e+01 rat_eff=7.0000e-01 inertia=1.0000e-01
  pi_2              dp=7.1379e-03
                    length=1.0000e+00 diam=1.0000e-01 area=7.8540e-03
                    rat_pf=1.0000e-04 rat_m=2.0000e+01
                    num_par=1
  valv_2            dp=1.8066e+00 pf=3.0058e-02
  pi_3              dp=5.0784e-03
                    length=1.0000e+00 diam=1.0000e-01 area=7.8540e-03
                    rat_pf=1.0000e-04 rat_m=3.0000e+01
                    num_par=1
  mx_1              diam=1.0000e-01 area=7.8540e-03
  gt_1              rpm=6.0000e+04 eff=8.0000e-01 power=8.1535e+06
                    rat_cmass=1.8256e+00 rat_cspeed=3.3490e+03
                    rat_pr=2.0000e+00 inertia=1.0000e+00
  valv_3            dp=1.1896e+00 pf=1.0000e-02
  valv_4            dp=5.8881e-01 pf=1.0000e-02
  pi_4              dp=4.2826e-03
                    length=1.0000e+00 diam=1.0000e-01 area=7.8540e-03
                    rat_pf=1.0000e-04 rat_m=2.0000e+01
                    num_par=1
  pi_5              dp=2.1198e-03
                    length=1.0000e+00 diam=1.0000e-01 area=7.8540e-03
                    rat_pf=1.0000e-04 rat_m=2.0000e+01
                    num_par=1
  htss_1            heat=1.8676e+09
  exnz_1            mreq=4.0000e+01 thrust=4.6046e+05 impulse=1.1747e+03
                    diam=2.1881e-01 area=3.7602e-02
                    aexp=4.7002e+00 eff=8.5000e-01
  rgen_1            tcomb=3.0000e+03 rat_m=1.2000e+01
```

Bleed Cycle (Uncooled Nozzle) — 150 MW PBR

thermodynamic data for HYDROGEN with flow id = THR-tH2
pc=12.800000, tc=33.200000, tb=20.400000, molwt=2.016000

task: sta n=0 f=2.406347e+05
  x= 1.000000e-01 1.000000e-01 1.000000e-02
  c=-2.220653e+00 -1.006090e+03 2.406326e+05
  h= 2 8380e-03 hs= 2.8380e-03 mu=2.50e+00 n=1.61e-02 s=1.11e-03 a=4.30e-01

task: sta n=1 f=8.395095e+05
  x= 1.292678e-01 4.651290e-02 1.815817e-02
  c=-8.480559e-01 -3.708270e+02 8.395094e+05
  h= 5.5454e-04 hs= 5.5454e-04 mu=1.50e+00 n=2.17e-03 s=1.46e-04 a=5.97e-01

task: sta n=2 f=5.195484e+05
  x= 1.483032e-01 6.917974e-04 1.394050e-02
  c= 1.934248e-01 1.577007e+03 5.195460e+05
  h= 3.5964e-03 hs= 5.5454e-04 mu=2.50e+00 n=2.22e-04 s=2.48e-05 a=5.73e-01

task: sta n=3 f=6.815490e+05
  x= 1.328687e-01 4.793099e-02 1.585148e-02
  c=-6.257368e-01 -4.738915e+02 6.815489e+05
  h= 5.3214e-04 hs= 5 3214e-04 mu=1.50e+00 n=8.75e-04 s=2.49e-05 a=3.98e-01

task: sta n=4 f=5.358772e+05
  x= 1.422617e-01 6.820045e-03 1.385938e-02
  c=-1.674903e-01 8.121051e+02 5.358766e+05
  h= 1.0068e-03 hs= 5.3214e-04 mu=2.50e+00 n=1.91e-04 s=1.39e-05 a=4.27e-01

task: sta n=5 f=5.938319e+05
  x= 1.357105e-01 3.900726e-02 1.449258e-02
  c=-4.917480e-01 -3.971147e+02 5.938318e+05
  h= 3.7022e-04 hs= 3.7022e-04 mu=1.50e+00 n=3.73e-04 s=1.24e-05 a=3.67e-01

task: sta n=6 f=4.395793e+05
  x= 1.413388e-01 9.832035e-03 1.234255e-02
  c=-2.205903e-01 4.879152e+02 4.395790e+05
  h= 3.9423e-04 hs= 3.7022e-04 mu=2.50e+00 n=1.34e-04 s=7.54e-06 a=3.80e-01

task: sta n=7 f=5.119306e+05
  x= 1.377990e-01 3.123783e-02 1.325884e-02
  c=-3.919973e-01 -3.063907e+02 5.119305e+05
  h= 2.3473e-04 hs= 2.3473e-04 mu=1.50e+00 n=1.88e-04 s=5.61e-06 a=3.49e-01

task: sta n=8 f=3.637987e+05
  x= 1.416273e-01 1.180677e-02 1.118610e-02
  c=-2.012424e-01 2.820718e+02 3.637986e+05
  h= 1.5367e-04 hs= 1.5367e-04 mu=5.04e-01 n=3.45e-05 s=3.44e-06 a=4.06e-01

task: sta n=9 f=9.089138e+04
  x= 1.428606e-01 2.068497e-02 7.167763e-03
  c=-1.136210e-01 -4.286157e+02 9.089037e+04
  h= 2.6593e-04 hs= 1.5367e-04 mu=1.50e+00 n=4.67e-05 s=1.88e-06 a=2.53e-01

task: sta n=10 f=2.039835e+05
  x= 1.429456e-01 1.197333e-02 8.845784e-03
  c=-1.218321e-01 9.834320e+01 2.039835e+05
  h= 2.7156e-05 hs= 2.7156e-05 mu=5.04e-01 n=1.40e-05 s=2.68e-07 a=2.41e-01

task: sta n=11 f=5.058146e+04
  x= 1.444591e-01 1.020737e-02 6.639716e-03

```
   c=-3.270680e-02   6.432010e+00   5.058146e+04
   h= 9.2963e-07 hs= 9.2963e-07 mu=0.00e+00 n=9.10e-07 s=2.47e-09 a=4.05e-01

 task: sta  n=12  f=5.614124e+02
   x= 1.450441e-01   8.937127e-03   5.915645e-03
   c= 1.308434e-03   2.006189e+01  -5.610538e+02
   h= 5.7115e-07 hs= 5.7115e-07 mu=0.00e+00 n=1.31e-08 s=9.72e-09 a=8.67e-01

 task: sta  n=13  f=3.862317e+02
   x= 1.449884e-01   9.544179e-03   5.921620e-03
   c=-1.514550e-03  -2.738197e+01   3.852599e+02
   h= 1.0636e-06 hs= 5.7115e-07 mu=1.00e+00 n=2.40e-09 s=2.20e-09 a=9.59e-01

 task: sta  n=14  f=4.667075e+02
   x= 1.450209e-01   9.188869e-03   5.913711e-03
   c= 1.218807e-04  -5.846959e-01  -4.667072e+02
   h= 5.3734e-10 hs= 5.3734e-10 mu=0.00e+00 n=5.03e-11 s=1.77e-12 a=2.08e-01

 task: sta  n=15  f=4.307005e+00
   x= 1.450190e-01   9.182303e-03   5.920483e-03
   c= 7.041374e-06   7.716100e-01  -4.237323e+00
   h= 8.4410e-10 hs= 5.3734e-10 mu=1.00e+00 n=5.11e-11 s=1.55e-12 a=1.91e-01

 task: sta  n=16  f=2.176135e+02
   x= 1.450199e-01   9.187595e-03   5.917330e-03
   c= 6.499601e-05  -3.834473e-02  -2.176135e+02
   h= 1.3815e-11 hs= 1.3815e-11 mu=0.00e+00 n=1.16e-11 s=7.45e-15 a=1.54e-01

 task: sta  n=17  f=5.189261e-01
   x= 1.450187e-01   9.191992e-03   5.920428e-03
   c=-3.075895e-06  -8.895801e-03   5.188498e-01
   h= 1.1492e-13 hs= 1.1492e-13 mu=0.00e+00 n=1.46e-15 s=3.62e-16 a=5.07e-01

 task: sta  n=18  f=1.810299e-01
   x= 1.450187e-01   9.191946e-03   5.920424e-03
   c=-8.789193e-07  -5.720998e-03   1.809394e-01
   h= 4.6627e-14 hs= 4.6627e-14 mu=0.00e+00 n=6.07e-16 s=1.89e-16 a=5.63e-01

 task: sta  n=19  f=4.297732e-02
   x= 1.450187e-01   9.191855e-03   5.920422e-03
   c= 2.155883e-07   1.266565e-03  -4.295865e-02
   h= 2.2878e-15 hs= 2.2878e-15 mu=0.00e+00 n=2.15e-17 s=8.05e-18 a=6.16e-01

 task: sta  n=20  f=5.999307e-04
   x= 1.450187e-01   9.191872e-03   5.920422e-03
   c= 3.010371e-09   1.768163e-05  -5.996700e-04
```

                    output of model flows

model	temp	pres	mass	enth	entr	dens	velc	qual
gas_1	20.0	0.99	3.800	-4.1280e+06	-1.0589e+05	7.712e+01	25.1	0.00
valv_1	19.9	0.89	3.800	-4.1280e+06	-1.0575e+05	7.731e+01	25.1	0.00
pi_1	19.9	0.89	3.800	-4.1280e+06	-1.0575e+05	7.731e+01	25.0	0.00
pump_1	32.6	60.10	3.800	-4.0171e+06	-1.0374e+05	6.692e+01	25.0	1.00
sp_1	32.6	60.10	3.765	-4.0171e+06	-1.0374e+05	6.692e+01	28.7	1.00
pi_2	32.6	60.10	3.765	-4.0171e+06	-1.0374e+05	6.692e+01	28.7	1.00
htss_1	3000.0	57.09	3.765	4.3764e+07	-2.9019e+04	4.657e-01	28.7	1.00
sp_2	3000.0	57.09	3.743	4.3764e+07	-2.9019e+04	4.657e-01	845.7	1.00
exnz_1	1094.1	0.31	3.743	1.1391e+07	-2.4287e+04	6.872e-03	8090.7	1.00
sp_1	32.6	60.10	0.035	-4.0171e+06	-1.0374e+05	6.692e+01	26.6	1.00
valv_2	32.6	51.39	0.035	-4.0171e+06	-1.0331e+05	6.483e+01	26.6	1.00
pi_3	32.6	51.38	0.035	-4.0171e+06	-1.0331e+05	6.483e+01	27.4	1.00
sp_2	3000.0	57.09	0.022	4.3764e+07	-2.9019e+04	4.657e-01	24.4	1.00
valv_4	3000.2	51.38	0.022	4.3764e+07	-2.8583e+04	4.193e-01	24.4	1.00
mx_1	1300.0	51.38	0.057	1.4597e+07	-4.2768e+04	9.636e-01	30.2	1.00

```
pi_4           1300.0  51.38   0.057   1.4597e+07  -4.2768e+04   9.635e-01    30.2   1.00
valv_3         1300.2  46.24   0.057   1.4597e+07  -4.2330e+04   8.677e-01    30.2   1.00
gt_1            814.6   4.62   0.057   7.2339e+06  -3.9873e+04   1.393e-01    30.2   1.00
exnz_2          677.9   2.43   0.057   5.2615e+06  -3.9873e+04   8.814e-02  1986.4   1.00

gas_1          diam=5.0000e-02 area=1.9635e-03
valv_1         dp=9.8692e-02 pf=1.0000e-01
pi_1           dp=8.8823e-05
               length=1.0000e+00 diam=5.0000e-02 area=1.9635e-03
               rat_pf=1.0000e-04 rat_m=3.8000e+00
               num_par=1
pump_1         rpm=3.0000e+04 dp=5.9216e+01 eff=7.0000e-01 power=-4.2129e+05
               rat_dp=5.9215e+01 rat_torque=1.3410e+02 rat_rpm=3.0000e+04
               rat_m=3.8000e+00 rat_eff=7.0000e-01 inertia=1.0000e-01
pi_2           dp=5.9004e-03
               length=1.0000e+00 diam=5.0000e-02 area=1.9635e-03
               rat_pf=1.0000e-04 rat_m=3.8000e+00
               num_par=1
htss_1         heat=1.7990e+08
sp_2           sr=5.9204e-03
               diam0=1.1000e-01 diam1=5.0000e-02 area0=9.5033e-03 area1=1.9635e-03
exnz_1         mreq=3.7428e+00 thrust=4.3219e+04 impulse=1.1783e+03
               diam=6.5192e-02 area=3.3379e-03
               aexp=4.1724e-01 eff=8.5000e-01
valv_2         dp=8.7162e+00 pf=1.4502e-01
pi_3           dp=3.9185e-03
               length=1.0000e+00 diam=5.0000e-03 area=1.9635e-05
               rat_pf=1.0000e-04 rat_m=4.0000e-02
               num_par=1
mx_1           diam=5.0000e-02 area=1.9635e-03
pi_4           dp=2.6287e-03
               length=1.0000e+00 diam=5.0000e-02 area=1.9635e-03
               rat_pf=1.0000e-04 rat_m=8.0000e-02
               num_par=1
valv_3         dp=5.1381e+00 pf=1.0000e-01
gt_1           rpm=3.0000e+04 eff=8.0000e-01 power=4.2129e+05
               rat_cmass=4.4618e-02 rat_cspeed=8.3198e+02
               rat_pr=1.0000e+01 inertia=1.0000e+00
exnz_2         mreq=5.7220e-02 thrust=1.9425e+02 impulse=3.4641e+02
               diam=2.0399e-02 area=3.2682e-04
               aexp=3.2682e-04 eff=6.0000e-01
sp_1           sr=9.1919e-03
               diam0=5.0000e-02 diam1=5.0000e-03 area0=1.9635e-03 area1=1.9635e-05
shft_1         rpm=3.0000e+04 power=-5.9967e-04 inertia=1.1000e+00
valv_4         dp=5.7093e+00 pf=1.0000e-01
```

Bleed Cycle (Cooled Nozzle) - 150 MW PBR

thermodynamic data for HYDROGEN with flow id = THR-tH2
pc=12.800000, tc=33.200000, tb=20.400000, molwt=2.016000

```
 ***WARNING: Design nozzle temp at section 09 is
             Exhaust side= 8.5216e+02  Space side= 7.2218e+01


task: sta   n=0  f=5.857797e+05
  x= 1.000000e-01  1.000000e-01  1.000000e-01  1.000000e-02
  c=-5.653663e+00 -4.984248e+00 -3.753869e+02  5.857796e+05

 ***WARNING: Design nozzle temp at section 09 is
             Exhaust side= 8.5216e+02  Space side= 7.2218e+01


 ***WARNING: Design nozzle temp at section 09 is
             Exhaust side= 8.5216e+02  Space side= 7.2218e+01


 ***WARNING: Design nozzle temp at section 09 is
             Exhaust side= 8.5216e+02  Space side= 7.2218e+01


 ***WARNING: Design nozzle temp at section 09 is
             Exhaust side= 8.5216e+02  Space side= 7.2218e+01

  h= 1.6014e-02 hs= 1.6014e-02 mu=0.00e+00 n=1.12e-02 s=9.47e-03 a=9.71e-01 b=2

 ***WARNING: Design nozzle temp at section 09 is
             Exhaust side= 8.5216e+02  Space side= 7.2218e+01


task: sta   n=1  f=5.491736e+05
  x= 1.498879e-01  1.226599e-02  9.586996e-02  9.738471e-03
  c=-3.804860e-01  2.347105e-01 -3.686160e+02  5.491735e+05
  h= 2.1791e-04 hs= 2.1791e-04 mu=0.00e+00 n=1.67e-04 s=1.22e-04 a=9.53e-01 b=2 b=2

 ***WARNING: Design nozzle temp at section 09 is
             Exhaust side= 8.5216e+02  Space side= 7.2218e+01


task: sta   n=2  f=2.098274e+05
  x= 1.480515e-01  9.240380e-03  2.094604e-02  9.993221e-03
  c=-1.986345e-01  1.024427e-01  4.848148e+02  2.098268e+05
  h= 1.9035e-04 hs= 1.9035e-04 mu=1.00e+00 n=8.08e-05 s=1.94e-05 a=6.03e-01

 ***WARNING: Design nozzle temp at section 09 is
             Exhaust side= 8.5216e+02  Space side= 7.2218e+01


task: sta   n=3  f=1.236275e+05
  x= 1.460157e-01  7.910180e-03  5.848510e-02  6.060316e-03
  c=-1.186839e-01  4.932442e-02 -3.535085e+02  1.236270e+05
  h= 9.6635e-05 hs= 9.6635e-05 mu=0.00e+00 n=1.23e-05 s=5.31e-06 a=6.99e-01

 ***WARNING: Design nozzle temp at section 09 is
             Exhaust side= 8.5216e+02  Space side= 7.2218e+01


task: sta   n=4  f=7.466618e+02
```

```
x= 1.447520e-01  5.935541e-03  3.375296e-02  5.991438e-03
c=-8.135714e-12 -1.679779e-03 -1.035468e+02  7.394470e+02
h= 7.6122e-06 hs= 7.6122e-06 mu=0.00e+00 n=5.64e-07 s=5.60e-07 a=9.97e-01

 ***WARNING: Design nozzle temp at section 09 is
             Exhaust side= 8.5216e+02  Space side= 7.2218e+01


task: sta  n=5  f=2.126762e+02
  x= 1.448769e-01  5.935541e-03  2.786511e-02  6.396649e-03
  c= 3.694822e-13  1.597163e-03  3.759019e+01 -2.093279e+02
  h= 1.0038e-06 hs= 1.0038e-06 mu=0.00e+00 n=4.03e-08 s=3.99e-08 a=9.95e-01

 ***WARNING: Design nozzle temp at section 09 is
             Exhaust side= 8.5216e+02  Space side= 7.2218e+01


task: sta  n=6  f=5.915901e+01
  x= 1.448318e-01  5.935541e-03  2.941759e-02  6.289199e-03
  c=-2.842171e-14 -7.376115e-05 -2.740351e+00  5.909550e+01
  h= 5.3332e-09 hs= 5.3332e-09 mu=0.00e+00 n=1.86e-10 s=1.84e-10 a=9.97e-01

 ***WARNING: Design nozzle temp at section 09 is
             Exhaust side= 8.5216e+02  Space side= 7.2218e+01


task: sta  n=7  f=4.161377e-01
  x= 1.448343e-01  5.935541e-03  2.930874e-02  6.296130e-03
  c= 0.000000e+00  1.239004e-06 -4.331299e-02  4.138775e-01
  h= 1.3322e-12 hs= 1.3322e-12 mu=0.00e+00 n=4.87e-14 s=4.75e-14 a=9.89e-01

 ***WARNING: Design nozzle temp at section 09 is
             Exhaust side= 8.5216e+02  Space side= 7.2218e+01


task: sta  n=8  f=8.344490e-03
  x= 1.448343e-01  5.935541e-03  2.930698e-02  6.296250e-03
  c= 0.000000e+00 -2.901758e-08  1.073151e-03  8.275195e-03
  h= 8.1779e-16 hs= 8.1779e-16 mu=0.00e+00 n=2.85e-17 s=2.78e-17 a=9.89e-01

 ***WARNING: Design nozzle temp at section 09 is
             Exhaust side= 8.5216e+02  Space side= 7.2218e+01


task: sta  n=9  f=4.801239e-04
  x= 1.448343e-01  5.935541e-03  2.930702e-02  6.296247e-03
  c= 0.000000e+00  1.287468e-09  6.601619e-06 -4.800785e-04
```

                    output of model flows

model	temp	pres	mass	enth	entr	dens	velc	qual
gas_1	20.0	0.99	3.800	-4.1280e+06	-1.0589e+05	7.712e+01	25.1	0.00
valv_1	19.9	0.89	3.800	-4.1280e+06	-1.0575e+05	7.731e+01	25.1	0.00
pi_1	19.9	0.89	3.800	-4.1280e+06	-1.0575e+05	7.731e+01	25.0	0.00
pump_1	32.6	60.10	3.800	-4.0171e+06	-1.0374e+05	6.692e+01	25.0	1.00
sp_3	32.6	60.10	1.900	-4.0171e+06	-1.0374e+05	6.692e+01	14.5	1.00
pump_2	37.0	99.58	1.900	-3.9317e+06	-1.0235e+05	6.817e+01	14.5	1.00
pi_2	37.0	99.58	1.900	-3.9317e+06	-1.0235e+05	6.817e+01	14.2	1.00
rgen_1	462.6	59.75	1.900	2.2476e+06	-5.8489e+04	3.112e+00	14.2	1.00
sp_1	462.6	59.75	1.844	2.2476e+06	-5.8489e+04	3.112e+00	301.8	1.00
sp_3	32.6	60.10	1.900	-4.0171e+06	-1.0374e+05	6.692e+01	1446.1	1.00
valv_5	32.6	59.75	1.900	-4.0171e+06	-1.0373e+05	6.686e+01	1446.1	1.00
mx_2	231.0	59.75	3.744	-9.3134e+05	-6.8041e+04	6.216e+00	306.8	1.00
htss_1	3000.0	56.76	3.744	4.3763e+07	-2.8995e+04	4.630e-01	306.8	1.00
sp_2	3000.0	56.76	3.721	4.3763e+07	-2.8995e+04	4.630e-01	845.7	1.00

```
exnz_1    1094.1   0.30   3.721  1.1391e+07 -2.4263e+04  6.832e-03 8090.7  1.00
sp_1       462.6  59.75   0.056  2.2476e+06 -5.8489e+04  3.112e+00  911.2  1.00
valv_2     462.7  51.09   0.056  2.2476e+06 -5.7833e+04  2.669e+00  911.2  1.00
pi_3       462.7  51.08   0.056  2.2476e+06 -5.7832e+04  2.668e+00 1062.9  1.00
sp_2      3000.0  56.76   0.024  4.3763e+07 -2.8995e+04  4.630e-01   25.9  1.00
valv_4    3000.2  51.08   0.024  4.3763e+07 -2.8559e+04  4.168e-01   25.9  1.00
mx_1      1300.0  51.08   0.079  1.4596e+07 -4.2744e+04  9.580e-01   42.1  1.00
pi_4      1300.0  51.08   0.079  1.4596e+07 -4.2743e+04  9.579e-01   42.1  1.00
valv_3    1300.2  45.97   0.079  1.4596e+07 -4.2305e+04  8.627e-01   42.1  1.00
gt_1       814.6   4.60   0.079  7.2339e+06 -3.9849e+04  1.385e-01   42.1  1.00
exnz_2     678.0   2.42   0.079  5.2618e+06 -3.9849e+04  8.763e-02 1986.4  1.00


gas_1       diam=5.0000e-02 area=1.9635e-03
valv_1      dp=9.8692e-02 pf=1.0000e-01
pi_1        dp=8.8823e-05
            length=1.0000e+00 diam=5.0000e-02 area=1.9635e-03
            rat_pf=1.0000e-04 rat_m=3.8000e+00
            num_par=1
pump_1      rpm=3.0000e+04 dp=5.9216e+01 eff=7.0000e-01 power=-4.2129e+05
            rat_dp=5.9215e+01 rat_torque=1.3410e+02 rat_rpm=3.0000e+04
            rat_m=3.8000e+00 rat_eff=7.0000e-01 inertia=1.0000e-01
pi_2        dp=2.4895e-03
            length=1.0000e+00 diam=5.0000e-02 area=1.9635e-03
            rat_pf=1.0000e-04 rat_m=3.8000e+00
            num_par=1
rgen_1      tcomb=3.0000e+03 rat_m=1.9000e+00
htss_1      heat=1.6735e+08
sp_2        sr=6.2962e-03
            diam0=1.1000e-01 diam1=5.0000e-02 area0=9.5033e-03 area1=1.9635e-03
exnz_1      mreq=3.7207e+00 thrust=4.2965e+04 impulse=1.1783e+03
            diam=6.5190e-02 area=3.3377e-03
            aexp=4.1722e-01 eff=8.5000e-01
valv_2      dp=8.6535e+00 pf=1.4483e-01
pi_3        dp=9.9015e-03
            length=1.0000e+00 diam=5.0000e-03 area=1.9635e-05
            rat_pf=1.0000e-04 rat_m=4.0000e-02
            num_par=1
mx_1        diam=5.0000e-02 area=1.9635e-03
pi_4        dp=5.0141e-03
            length=1.0000e+00 diam=5.0000e-02 area=1.9635e-03
            rat_pf=1.0000e-04 rat_m=8.0000e-02
            num_par=1
valv_3      dp=5.1079e+00 pf=1.0000e-01
gt_1        rpm=3.0000e+04 eff=8.0000e-01 power=5.8354e+05
            rat_cmass=6.2168e-02 rat_cspeed=8.3198e+02
            rat_pr=1.0000e+01 inertia=1.0000e+00
exnz_2      mreq=7.9258e-02 thrust=2.6907e+02 impulse=3.4641e+02
            diam=2.4078e-02 area=4.5533e-04
            aexp=4.5533e-04 eff=6.0000e-01
sp_1        sr=2.9307e-02
            diam0=5.0000e-02 diam1=5.0000e-03 area0=1.9635e-03 area1=1.9635e-05
shft_1      rpm=3.0000e+04 power=0.0000e+00 inertia=0.0000e+00
valv_4      dp=5.6760e+00 pf=1.0000e-01
sp_3        sr=5.0000e-01
            diam0=5.0000e-02 diam1=5.0000e-03 area0=1.9635e-03 area1=1.9635e-05
pump_2      rpm=3.0000e+04 dp=3.9477e+01 eff=7.0000e-01 power=-1.6225e+05
            rat_dp=3.9477e+01 rat_torque=5.1645e+01 rat_rpm=3.0000e+04
            rat_m=1.9000e+00 rat_eff=7.0000e-01 inertia=1.0000e-01
mx_2        diam=5.0000e-02 area=1.9635e-03
valv_5      dp=3.5675e-01 pf=5.9355e-03
```

EXPANDER CYCLE - 150 MW PBR

thermodynamic data for HYDROGEN with flow id = THR-tH2
pc=12.800000, tc=33.200000, tb=20.400000, molwt=2.016000

  ***WARNING: Design nozzle temp at section 09 is
              Exhaust side= 8.5613e+02 Space side= 7.7407e+01

task: sta   n=0   f=1.162917e+00
  x= 1.000000e-02 3.000000e+03
  c= 1.162917e+00 0.000000e+00

  ***WARNING: Design nozzle temp at section 09 is
              Exhaust side= 8.5613e+02 Space side= 7.7407e+01

  ***WARNING: Design nozzle temp at section 09 is
              Exhaust side= 8.5613e+02 Space side= 7.7407e+01

  h= 3.7440e-04 hs= 3.7440e-04 mu=0.00e+00 n=3.74e-04 s=3.74e-04 a=1.00e+00

  ***WARNING: Design nozzle temp at section 09 is
              Exhaust side= 8.5613e+02 Space side= 7.7407e+01

task: sta   n=1   f=2.955424e-09
  x= 2.934936e-02 3.000000e+03
  c=-2.955424e-09 0.000000e+00

output of model flows

model	temp	pres	mass	enth	entr	dens	velc	qual
gas_1	20.0	0.99	3.800	-4.1280e+06	-1.0589e+05	7.712e+01	25.1	0.00
valv_1	19.9	0.89	3.800	-4.1280e+06	-1.0575e+05	7.731e+01	25.1	0.00
pi_1	19.9	0.89	3.800	-4.1280e+06	-1.0575e+05	7.731e+01	25.0	0.00
pump_1	32.6	60.10	3.800	-4.0171e+06	-1.0374e+05	6.692e+01	25.0	1.00
sp_1	32.6	60.10	1.900	-4.0171e+06	-1.0374e+05	6.692e+01	14.5	1.00
pump_2	42.1	148.93	1.900	-3.8250e+06	-1.0091e+05	6.943e+01	14.5	1.00
pi_2	42.1	148.89	1.900	-3.8250e+06	-1.0091e+05	6.943e+01	13.9	1.00
rgen_1	467.2	89.33	1.900	2.3171e+06	-6.0039e+04	4.563e+00	13.9	1.00
pi_4	467.2	89.31	1.900	2.3171e+06	-6.0037e+04	4.562e+00	212.1	1.00
valv_3	467.2	88.41	1.900	2.3171e+06	-5.9995e+04	4.518e+00	212.1	1.00
gt_1	424.2	58.94	1.900	1.7155e+06	-5.9635e+04	3.346e+00	212.1	1.00
pi_5	424.2	58.93	1.900	1.7155e+06	-5.9634e+04	3.345e+00	289.3	1.00
valv_4	424.2	58.34	1.900	1.7155e+06	-5.9591e+04	3.313e+00	289.3	1.00
sp_1	32.6	60.10	1.900	-4.0171e+06	-1.0374e+05	6.692e+01	14.5	1.00
valv_2	32.6	58.34	1.900	-4.0171e+06	-1.0367e+05	6.660e+01	11.5	1.00
pi_3	32.6	58.34	1.900	-4.0171e+06	-1.0367e+05	6.660e+01	14.5	1.00
mx_1	214.9	58.34	3.800	-1.1508e+06	-6.8931e+04	6.534e+00	296.2	1.00
htss_1	3000.0	55.42	3.800	4.3762e+07	-2.8897e+04	4.521e-01	296.2	1.00
exnz_1	1086.8	0.29	3.800	1.1281e+07	-2.4162e+04	6.548e-03	8065.4	1.00

gas_1	diam=5.0000e-02 area=1.9635e-03
valv_1	dp=9.8692e-02 pf=1.0000e-01
pi_1	dp=8.8823e-05
	length=1.0000e+00 diam=5.0000e-02 area=1.9635e-03
	rat_pf=1.0000e-04 rat_m=3.8000e+00
	num_par=1
pump_1	rpm=3.0000e+04 dp=5.9216e+01 eff=7.0000e-01 power=-4.2129e+05
	rat_dp=5.9215e+01 rat_torque=1.3410e+02 rat_rpm=3.0000e+04

```
                   rat_m=3.8000e+00 rat_eff=7.0000e-01 inertia=1.0000e-01
  sp_1             sr=5.0000e-01
                   diam0=5.0000e-02 diam1=5.0000e-02 area0=1.9635e-03 area1=1.9635e-03
  shft_1           rpm=3.0000e+04 power=0.0000e+00 inertia=0.0000e+00
  pump_2           rpm=3.0000e+04 dp=8.8824e+01 eff=7.0000e-01 power=-3.6506e+05
                   rat_dp=8.8823e+01 rat_torque=1.1620e+02 rat_rpm=3.0000e+04
                   rat_m=1.9000e+00 rat_eff=7.0000e-01 inertia=1.0000e-01
  pi_2             dp=4.1369e-02
                   length=1.0000e+00 diam=5.0000e-02 area=1.9635e-03
                   rat_pf=1.0000e-04 rat_m=1.1400e+00
                   num_par=1
  valv_2           dp=1.7640e+00 pf=2.9349e-02
  pi_3             dp=2.9765e-03
                   length=1.0000e+00 diam=5.0000e-02 area=1.9635e-03
                   rat_pf=1.0000e-04 rat_m=2.6600e+00
                   num_par=1
  mx_1             diam=5.0000e-02 area=1.9635e-03
  gt_1             rpm=3.0000e+04 eff=8.0000e-01 power=1.1430e+06
                   rat_cmass=4.6449e-01 rat_cspeed=1.3879e+03
                   rat_pr=1.5000e+00 inertia=1.0000e+00
  valv_3           dp=8.9307e-01 pf=1.0000e-02
  valv_4           dp=5.8926e-01 pf=1.0000e-02
  pi_4             dp=2.4814e-02
                   length=1.0000e+00 diam=5.0000e-02 area=1.9635e-03
                   rat_pf=1.0000e-04 rat_m=1.1400e+00
                   num_par=1
  pi_5             dp=1.6373e-02
                   length=1.0000e+00 diam=5.0000e-02 area=1.9635e-03
                   rat_pf=1.0000e-04 rat_m=1.1400e+00
                   num_par=1
  htss_1           heat=1.7067e+08
  exnz_1           mreq=3.8000e+00 thrust=4.3744e+04 impulse=1.1747e+03
                   diam=6.7416e-02 area=3.5696e-03
                   aexp=4.4620e-01 eff=8.5000e-01
  rgen_1           tcomb=3.0000e+03 rat_m=1.9000e+00
```

For a single stage rocket

$$\Delta V = c \ln \frac{m_o}{m_f} \qquad (\text{Ref } 1, \, p99)$$

$$I_{sp} = \frac{\dot{m} c}{\dot{m} g} \qquad (\text{Ref } 1, \, p22)$$

$$\ln \frac{m_o}{m_f} = \frac{\Delta V}{I_{sp} \cdot g}$$

for equal ΔV

$$I_{sp_1} \cdot g \cdot \ln \frac{m_o}{m_f}\bigg|_1 = I_{sp_2} \cdot g \cdot \ln \frac{m_o}{m_f}\bigg|_2$$

$$\ln \frac{m_o}{m_f}\bigg|_2 = \frac{I_{sp_1}}{I_{sp_2}} \cdot \ln \frac{m_o}{m_f}\bigg|_1$$

$$\frac{m_o}{m_f}\bigg|_2 = \left(\frac{m_o}{m_f}\bigg|_1\right)^{\frac{I_{sp_1}}{I_{sp_2}}}$$

for Mars mission

$$\Delta V \simeq 20 \text{ km/sec} = 20000 \text{ m/sec}$$

$I_{sp} = 1175$ for Expander cycle

$$\frac{m_o}{m_c}\bigg|_{exp} = 5.669 \implies \text{Normalized ignition mass} = 1.0$$

$I_{sp} = 1153$ for Bleed cycle w/coded nozzle

$$\frac{m_o}{m_c}\bigg|_{blc} = 5.860 \implies \text{Norm. ign. mass} = 1.034$$

$I_{sp} = 1157$ for Bleed cycle w/uncoded nozzle

$$\frac{m_o}{m_c}\bigg|_{bluc} = 5.824 \implies \text{Norm. ign. mass} = 1.027$$

for OTV mission
$$\Delta V \approx 14,000 \, {}^{ft}/_s = 4267 \, {}^m/s$$

$$\left. \frac{m_f}{m_o} \right|_{exp} = .6906 \Rightarrow \text{Normalized payload mass} = 1.0$$

$$\left. \frac{m_f}{m_o} \right|_{bl_c} = .6857 \Rightarrow \text{Norm. payload mass} = 0.993$$

$$\left. \frac{m_f}{m_o} \right|_{bl_{uc}} = .6871 \Rightarrow \text{Norm payload mass} = 0.995$$